Dear Author

Please use this PDF proof to check the layout of your article. If you would like any changes to be made to the layout, you can leave instructions in the online proofing interface. First, return to the online proofing interface by clicking "Edit" at the top page, then insert a Comment in the relevant location. Making your changes directly in the online proofing interface is the quickest, easiest way to correct and submit your proof.

Please note that changes made to the article in the online proofing interface will be added to the article before publication, but are not reflected in this PDF proof.

If you would prefer to submit your corrections by annotating the PDF proof, please download and submit an annotatable PDF proof by clicking the link below.

Annotate PDF

Computers and Chemical Engineering xxx (xxxx) xxx

Contents lists available at ScienceDirect

Computers and Chemical Engineering

journal homepage: www.elsevier.com/locate/compchemeng

Optimal design of ethylene and propylene coproduction plants with generalized disjunctive programming and state equipment network models

Q1 H.A. Pedrozo[a], S.B. Rodriguez Reartes[a,b], A.R. Vecchietti[c], M.S. Diaz[a,b,*], I.E. Grossmann[d]

[a] Planta Piloto de Ingeniería Química (PLAPIQUI CONICET-UNS), Camino La Carrindanga km. 7, Bahía Blanca, Argentina
[b] Departamento de Ingeniería Química, Universidad Nacional del Sur (UNS), Bahía Blanca, Argentina
[c] Institute of Design and Development (INGAR CONICET-UTN), Avellaneda 3657, Santa Fe, Argentina
[d] Department of Chemical Engineering, Carnegie Mellon University, 5000 Forbes Avenue, Pittsburgh, PA 15213, USA

ARTICLE INFO

Article history:
Received 19 December 2020
Revised 14 March 2021
Accepted 19 March 2021
Available online xxx

Keywords:
Olefin production
Superstructure optimization
Propane dehydrogenation
Metathesis
Steam cracking
State equipment network representation
Logic-based outer approximation algorithm
Generalized disjunctive programming

ABSTRACT

In this work, we propose a superstructure optimization approach for the optimal design of an ethylene and propylene coproduction plant. We formulate a superstructure that embeds ethane and propane steam cracking technologies, propane dehydrogenation and olefin metathesis processes. We represent the superstructure with a Generalized Disjunctive Programming model, and solve the problem through a custom implementation of the Logic-based Outer Approximation algorithm in GAMS. We propose a state-equipment-network representation to model potential distillation trains, as well as alternative acetylene reactor configurations. Rigorous models are formulated for distillation columns, compressors, turboexpanders, vessels and several process equipment units. The objective function is to maximize the net present value. We analyze four international price scenarios for raw material and utility costs, while considering global ethylene and propylene prices. We obtain the optimal scheme for each case. Numerical results show that the combination of ethane steam cracking, olefin metathesis and ethylene dimerization is the most profitable configuration under low ethane price scenarios, whereas the combination of ethane and propane steam cracking together with propane dehydrogenation is the optimal solution when the propane price is on the order of ethane price.

1. Introduction

The shale gas revolution has led to the availability of natural gas liquids (NGLs), which represent excellent feedstock for the chemical industry. In particular, there are economic advantages on using NLGs for olefin production instead of naphtha feedstock (Siirola, 2014). For this reason, there is a general trend to modify reactive furnaces to use ethane, instead of naphtha, for ethylene production (Jenkins, 2012), even in countries that import shale gas from other countries (U.S. Energy Information Administration, 2019). These feedstock and technology changes lead to propylene yield reduction, since in the naphtha cracking process, propylene selectivity is higher than in ethane steam cracking. Furthermore, propylene demand continues to rise mainly due to polypropylene consumption (Baker, 2018). The combination of both issues increases the need for special purpose technologies for propylene production (Lavrenov et al., 2015).

Several process alternatives have been proposed to produce propylene from both petrochemical raw materials and chemical intermediates, such as methanol into olefins (Tian et al., 2015), methanol into propylene (Ali et al., 2019; Koempel and Liebner, 2007), olefin metathesis (Mol, 2004), propane dehydrogenation (Nawaz, 2015) and deep catalytic cracking (Akah and Al-Ghrami, 2015). Among these alternatives, both propane dehydrogenation and olefin metathesis are particularly interesting technologies since they can be used synergistically with ethane steam cracking to produce ethylene and propylene more efficiently.

In order to obtain an optimal design of a plant producing olefins, mathematical optimization modeling approaches can be very effective. Diaz and Bandoni (Diaz and Bandoni, 1996) formulated an MINLP problem to make discrete decisions and to optimize the operating conditions in an ethane-based ethylene plant. Lee et al. (Lee et al., 2003) postulated a superstructure based on the state-task-network (Yeomans and Grossmann, 1999a) representation, and determined the optimal scheme that minimizes the cost of separating a given mixture of olefins. Onel, Niziolek, & Floudas (Onel et al., 2016) addressed the olefin production optimal design from natural gas, via methanol. Gong & You

* Corresponding author.
E-mail address: sdiaz@plapiqui.edu.ar (M.S. Diaz).

https://doi.org/10.1016/j.compchemeng.2021.107295
0098-1354/

Nomenclature

Functions

f^{CON}	Function to calculate the bubble point of the mixture
f^{cu}	Correlation to estimate cooling utilities cost
f^{EVA}	Function to calculate the dew point of the mixture
f^{hu}	Correlation to estimate heating utilities cost
f_r^k	Van 't Hoff equation to calculate the equilibrium constant of reaction r
f_j^{LIQ}	Polynomial function to calculate liquid enthalpy of pure component j from unit temperature
f_j^{pvap}	Extended Antoine equation to calculate the partial pressures of pure component j
f_j^{VAP}	Polynomial function to calculate vapor enthalpy of pure component j from unit temperature
f^{XE}	Surrogate model to calculate ethylene losses in acetylene reactor
g^u	Cost correlation of unit u

Variables

CC_u	capital cost associated to unit u
$CcUt_u$	cooling utility costs in unit u
$ChUt_u$	heating utility costs in unit u
$CInv$	Investment cost
$Cp_{u,j}$	specific heat of pure component j in unit u
Cpm_u	average specific heat in unit u
CRM_u	costs associated to raw material u
DPu_u	pressure drop in unit u
$DR_{u,n}$	the liquid to-vapor ratio in stage n of column u
$DV_{u,n}$	vapor flowrate from stage n in column u
eg_u	ratio between gas constant and average specific heat
$ElecT$	electricity annual cost of electricity
$F_{u1,u,j}$	molar flowrate of component j for the process stream that leaves $u1$ and enters u
$Fi_{j1,j}$	molar flowrate of component j that is fed to cracking furnaces operating with component $j1$
$Ftl_{u,u2,j}$	logarithmic transformations of the flowrate for reactive component
$H_{u1,u}$	enthalpy flow of process streams that leave unit $u1$ and enter unit u
Hi_{j1}	enthalpy flow that is fed to cracking furnaces operating with component $j1$
$Hj_{p,u,j}$	specific enthalpy in phase p of component j at output temperature of u
$H2C_u$	hydrogen flowrate entering the unit u
$KTeq_{u,r}$	natural logarithm of equilibrium constant of reaction r in unit u
$Lp_{u,j}$	natural logarithm of partial pressure of component j at output temperature of u
$P_{u1,u}$	pressure of process streams that leave unit $u1$ and enter unit u
PR_u	the pressure ratio of unit u
Q_u	heat duty of unit u
Qc_u	condenser duty of column u
Qf_u	overall heat exchanged in the furnace u
Qh_u	reboiler duty of column u
Rev_u	annual revenues for product u
$Rsp_{u,u2}$	split fraction of stream that goes from u to $u2$
$Stl_{u,j}$	output liquid flowrate of component j for unit u
$Stv_{u,j}$	output vapor flowrate of component j for unit u
$T_{u1,u}$	temperature of process stream that leave unit $u1$ and enter unit u
$Tcom_u$	average temperature for the compressor u
TI	total income
$Tiso_u$	isentropic temperature of unit u
Tu_u	output temperature of process stream that leave unit u
usg_u	vapor flow velocity in unit u
$Vlj_{u,j}$	liquid volume of component j evaluated at output temperature of unit u
Vl_u	liquid molar volume of output stream from unit u
Vv_u	vapor molar volume of output stream from unit u
W_u	work related to unit u
$x_{u1,u,j}$	molar fraction of component j for the process stream that leaves $u1$ and enters u
$xl_{u,j}$	liquid stream molar fraction for component j leaving unit u
XV_j	conversion of component j
$xv_{u,j}$	vapor stream molar fraction for component j leaving unit u

Boolean variables

Y_u	Boolean variable that is true if unit u is present
$YT_{u,t}$	Boolean variable that is true if task t is performed in unit u and false otherwise
Z_{PDC}	Boolean variable that is true if Catofin technology is selected in PDH unit
Z_{PDO}	Boolean variable that is true if Oleflex technology is selected in PDH unit

Parameters

$At_{j,a}$	number of atoms a in component j
$cf_{AN,j,i}$	component parameters of extended Antoine equation
$cf_{CP,j,i}$	polynomial coefficients to calculate specific heat and vapor enthalpy
$cf_{HL,j,i}$	polynomial coefficients to calculate liquid enthalpy
$cf_{VL,j,i}$	polynomial coefficients to calculate liquid volume
$CY_{u,j1,j}$	carbon yield of component j from reactive component $j1$ in unit u
H_j^0	component enthalpy evaluated at the reference temperature
HPY	working time per year
K_{sb}	Souders-Brown constant
MTS_j	selectivities towards higher alkenes j in the metathesis reactor
MW_j	molecular weight of component j
$PriceE$	electricity price
$Price_u$	product or raw material price
R	gas constant
$Tref$	reference temperature

Greek letters

ω	working capital cost fraction
α	annuity
β	contingency and fee factor
γ	maintenance cost fraction
η_u	isentropic efficiency of unit u
θ	interest rate
τ	total project life
σ	net benefits tax
φ	auxiliary facilities factor

Sets

AT	set of atoms
CCU	set of units that have an investment cost
CD_u	condenser stage in unit u

J	set of components
JDr	set of reactive components in the dimerization reactor
JIr	set of reactive components in the isomerization reactor
JMr	set of reactive components in the metathesis reactor
JPb	set of produced components in C4 hydrogenation (butenes and oligomers)
JRb	set of C4 diene and enyne compounds
Jr_u	subset of reactive component in unit u
NFe_u	contains pairs $(u1, n)$ such that the stream from unit $u1$ to column u enters in stage n
NS_u	separation stages in distillation column u
RB_u	reboiler stage in unit u
Ta_u	set of tasks that can be performed in unit u
U	set of units
Ucb_u	set of units describing combustion reaction outside the coils
$Ucomp$	set of compressor units
Ucu	subsets of units that require cooling utilities
Ud	subset of conditional units
Udc	set of distillation columns
Uds	set of disjunctive splitters
Uex	set of units excluded from material balance
Ufl	set of flash units
Uhu	subsets of units that require heating utilities
Uhx	set of heat exchanger
$Uhxc$	set of heat exchangers that deliver a liquid stream at its bubble point
$Uhxe$	set of heat exchangers that deliver a vapor stream at its dew point
$Uhxl$	set of liquid single phase heat exchangers
$Uhxv$	set of vapor single phase heat exchangers
$Uhxw$	set of vapor heat exchangers to ensure that operating pressure is lower than the dew point
Uis_u	set of pseudo-mixers that feed process unit u
UI_u	subset of units that has input flowrates to unit u
UL_u	subset of units to which liquid streams from unit u
Umt	set of units that are forced to be included when the metathesis section is selected
Umx	set of mixers
UO_u	subset of units that has output flowrates from unit u
Uos_u	set of pseudo-splitters that deliver an output stream from u
Upc	set of pressure changer units
Upd	set of products
Uqm	set of pairs of units that exchange heat
Ur	set of reactive units
Urm	set of raw materials
$Us^{in}_{u',u,t}$	state that is fed through pseudo-mixer u' and processed in unit u when task t is selected
$Us^{out}_{u,u',t}$	state that is delivered through pseudo-splitter u' and produced in unit u when task t is selected
Usc	set of units describing cracking reaction inside the coils
$USEN$	set of units that can perform different tasks
Usp	set of splitters
Ust	set of states
UV_u	subset of units to which vapor streams from unit u
$Uves$	set of vessels

Indices

j	index of component
m	index of physical change
p	index of phases
r	index of reactions
t	index of tasks
u	index of units

(Gong and You, 2018) studied the optimal design of an integrated shale gas separation and chemical manufacturing process by formulating a superstructure which includes steam cracking, oxidative dehydrogenation, and catalytic dehydrogenation as alternative technologies. The simultaneous optimal design of reactor networks and separation systems has been recently addressed (Kong and Maravelias, 2020a; Ryu et al., 2020). Andersen, Diaz, & Grossmann (Andersen et al., 2013) have proposed the optimal design of integrated ethanol and gasoline supply chain. Pedrozo et al.(Pedrozo et al., 2020) have proposed an algorithm for the optimal design of ethylene plants based on multivariable piecewise linear surrogate models.

NGLs-based olefin plants including propane dehydrogenation and olefin metathesis as alternatives have not been addressed in the current literature. Moreover, we should note that several process superstructure optimizations have been reported based on shortcut models for distillation columns (Kong and Maravelias, 2020b; Narváez-García et al., 2017). However, it is worth noting that even though these approaches allow simplifying the optimization model, they can introduce significant errors when compared to rigorous mass, equilibrium, summation and heat (MESH) equation models (Dowling and Biegler, 2015), and consequently, inaccurate estimations regarding economic performance can be obtained.

In this work, we propose a superstructure embedding different process technologies for an olefin plant applying the state equipment network (SEN) representation (Yeomans and Grossmann, 1999a), and rigorous equations (MESH) to model distillation columns taking into account the relevance of the separation scheme, as well as rigorous models for compressors, turboexpanders and several process equipment units. Ethane and propane steam cracking, propane dehydrogenation, and metathesis are considered as potential technologies for ethylene and propylene production. The model is formulated as a Generalized Disjunctive Programming (GDP) problem, which is solved with a custom implementation of the Logic-based Outer Approximation algorithm. Numerical results provide useful insights for integrated olefin plants, as several price scenarios are analyzed considering raw material and utility costs from the United States, the European Union, Russia and Argentina. Furthermore, we perform heat integration for the optimal configuration of each price scenario, and we assess the potential economic improvement.

2. Process description

The present work addresses the optimal design problem for the coproduction of ethylene and propylene based on shale gas, using ethane and propane as raw materials. The main difference between shale and natural gas is the ethane content, which is higher in shale gas. Furthermore, the existence of large reserves of shale gas in several countries leads to higher ethane availability and, consequently, lower ethane price. The different process alternatives consist of three main sections: alkane conversion, separation train and metathesis section, as is described in the following subsections (Fig. 1).

2.1. Alkane conversion

There are different technologies associated to different reactor networks for the transformation of ethane and/or propane into

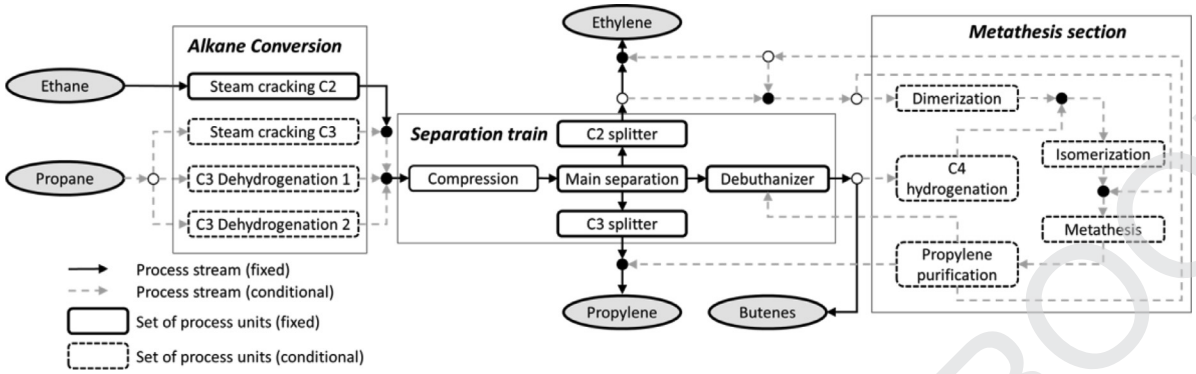

Fig. 1. Simplified superstructure of process alternatives.

olefins. In this work, we consider ethane and/or propane steam cracking and/or propane dehydrogenation.

2.1.1. Ethane conversion

The commercial technology to produce ethylene from ethane feedstock is steam cracking (SC) (Diaz and Bandoni, 1996; Schulz et al., 2000; Zimmermann and Walzl, 2009). Even though research on alternative reaction pathways to convert ethane to ethylene is an active area of research (Cavani et al., 2007; Gao et al., 2019; Pedrozo et al., 2020), the SC process is the commercial one being used, and its economic performance is difficult to challenge (Stangland, 2018).

2.1.2. Propane conversion

Several technologies have been developed for specifically producing propylene (Ondrey, 2014, 2004), as it was discussed in the Introduction section. In this work, we consider three different reaction pathways for handling propane feedstock, which are: propane steam cracking, Pt-based propane dehydrogenation, and Cr-based propane dehydrogenation.

Propane steam cracking mainly produces ethylene, with lower yields than with ethane feed (Zimmermann and Walzl, 2009). It requires complex furnace reactors operating at high temperatures, as in ethane steam cracking. Ethylene can be further used to produce propylene through a metathesis process. A second alternative that has proved to be commercially successful, has been developed by UOP Oleflex and it has propane conversions per pass of the order of 36 %, with 85 % propylene selectivity (Maddah, 2018). It employs a $Pt-Sn/Al_2O_3$-based catalyst, which is highly active and stable. A third alternative is the Catofin Process, in which a propane dehydrogenation unit has 40 % propane conversion per pass, and 88 % propylene selectivity (Maddah, 2018). A low cost catalyst is used that contains 18-20 % wt of CrO_x doped with 1-2 wt% of K or Na, and γ-Al_2O_3 as support (Sattler et al., 2014). There are more dehydrogenation technologies, with different catalysts that are not considered in this work.

2.2. Separation train

Since the output streams from ethane and propane conversion reactors mainly involve the same chemical components (H_2, CH_4, C_2H_4, C_2H_4, C_3H_6, C_3H_8, C_4^+), they are mixed and sent to the same separation train to purify the olefin products. Thus, this strategy leads to process intensification. Several authors describe the separation train downstream steam cracking processes (Borralho, 2013; Schulz et al., 2005; Verma and Hu, 2008; Zimmermann and Walzl, 2009). The initial feed conditioning mainly consists of a quench tower to cool the reactor outlet stream, a series of compression stages to increase the stream pressure, an acid gas removal unit to eliminate carbon dioxide and hydrogen sulfide, and a dehydration process. The conditioned stream is further processed in a reactor for acetylene hydrogenation, a cold box for hydrogen separation and ethylene recovery, and a sequence of distillation columns to perform product purification.

High energy savings can be achieved in this section, and there are several designs for this separation train aiming at economic improvement. The best option depends on the inlet stream composition, and they are mainly labeled by the first separation task. Thus, the main design configuration consists of demethanizer first, deethanizer first or depropanizer first scheme (Zimmermann and Walzl, 2009). The separation train also includes a debutanizer column, and ethane-ethylene and propane-propylene splitters. Ethane and propane are recycled to reactors in the alkane conversion section (see Fig. 1). The butane top stream from the debutanizer column can be either sold or fed to the Metathesis section, and a pyrolysis gasoline bottoms stream is sold as a byproduct.

2.3. Metathesis section

An alternative process to produce propylene is ethylene and butenes metathesis (Mazoyer et al., 2013). In this process, propylene selectivity is around 95 %, and butenes conversion per-pass is over 60 % (Ondrey, 2004). This technology employs a mixture of WO_3/SiO_2 and MgO, as catalysts for the metathesis and isomerization reactions, respectively (Mol, 2004). One important advantage associated to this process is that the reactor output stream does not contain ethane or propane. Therefore, distillation columns with a large number of trays are not required, and less energy is consumed to separate the olefin products.

Raw materials are ethylene and a butene mixture. Since the butene mixture stream is fed from the ethane and propane conversion section, it contains vinylacetylene, butylene, and isomers of 1-butene. For this reason, this stream is previously fed to a selective hydrogenation reactor to eliminate diene and enyne compounds (Koeppel et al., 1994). The outlet stream from this reactor is fed to an isomerization reactor to increase trans-2-butene content (Jiang et al., 2016). The outlet butene stream is mixed with ethylene and heated up to the reaction temperature, which is around 260 °C (Ondrey, 2004). The outlet stream is fed to a fixed bed catalytic reactor where the metathesis reaction takes place (Jiang et al., 2016). The metathesis reactor outlet stream is a mixture of ethylene, propylene, butenes, pentanes and heavier hydrocarbons. This stream is sent to a separation train, whose products are: ethylene, propylene and C_4^+. The ethylene stream can be recycled or mixed with the ethylene product stream; the propylene stream is mixed with the propylene stream product; and the C_4^+ stream is sent to the debutanizer column in the main separation train section. In this last process, referred to as "Propylene purification", there are discrete decisions regarding the separation sequence.

3. Methodology

3.1. Generalized disjunctive programming

In this work, we propose a superstructure optimization approach for the optimal design of an ethylene-propylene coproduction plant embedding models for the units described in Section 2. We represent the superstructure with a Generalized Disjunctive Programming (GDP) model (Chen et al., 2018; Trespalacios and Grossmann, 2014; Vecchietti and Grossmann, 2000), in which the presence of process units is associated to Boolean variables. Its general formulation is as follows,

$$
\begin{aligned}
&(\mathrm{P}-\mathrm{GDP}):\\
&\max NPV = f(x)\\
&s.t.\, g(x) \le 0\\
&\begin{bmatrix} Y_u \\ h_u(x) \le 0 \\ A_u x \le b \end{bmatrix} \veebar \begin{bmatrix} \neg Y_u \\ B_u x = 0 \end{bmatrix} u \epsilon Ud\\
&\bigvee_{t \epsilon Ta_u} \begin{bmatrix} YT_{u,t} \\ C_{u,t} x = 0 \end{bmatrix} u \epsilon USEN\\
&\Omega(Y_u, YT_{u,t}) = True\\
&x \epsilon X \subseteq \mathbb{R}^n\\
&Y_u \epsilon \{True, False\}\ u \epsilon Ud\\
&YT_{u,t} \epsilon \{True, False\}\ t \epsilon Ta_u\ u \epsilon USEN
\end{aligned}
$$

The objective function is the net present value (NPV) maximization, subject to general equations, disjunctions for units, disjunctions for the state equipment network (SEN) representation of distillation columns and logical equations. Y_u is the Boolean variable that is true if unit u is selected, and false otherwise; $YT_{u,t}$ is the Boolean variable that is true if task t is performed in unit u, and false otherwise; and x are continuous variables that include material flows, operating temperatures and pressures, enthalpy flows, unit internal variables, and capital costs; Ud is the subset of conditional units; $USEN$ is the set of units that can perform different tasks; and Ta_u is the set of tasks that can be performed in unit u.

To solve the complex GDP problem, we have implemented the Logic-based Outer Approximation algorithm (Chen et al., 2018; Türkay and Grossmann, 1996; Vecchietti and Grossmann, 2000) within the modeling environment GAMS (Rosenthal, 2014), as described in Section 3.3.

3.2. State equipment network

We propose a state-equipment-network (SEN) approach to model potential distillation trains, as well as alternative acetylene reactor configurations. The main separation train is a critical part of the process economics. Due to the combinatorial alternatives, the problem complexity increases with the number of units and tasks included in the superstructure. Yeomans and Grossmann (Yeomans and Grossmann, 1999a) have proposed the state-equipment-network (SEN) representation, which allows a systematic problem formulation. These authors also proposed the state-task-network (STN) approach (Yeomans and Grossmann, 1999a). However, we select the SEN representation because it requires fewer equipment units and leads to a smaller problem than STN, and it is more suitable for rigorous distillation sequences (Yeomans and Grossmann, 2000). For instance, the superstructure of a distillation train to separate four components includes ten columns for the STN representation, while the formulation with SEN requires three columns for the same separation train. Furthermore, in SEN representation, predefined and non-existent process units are avoided since the number of units depends on the number of components to be separated. Consequently, the number of flow and size variables forced to be zero is reduced, and the potential issues regarding singularities are also reduced (Kocis and Grossmann, 1989; Türkay and Grossmann, 1996). In SEN, the feed and produced states of equipment units depend on potential tasks that can be performed in each unit.

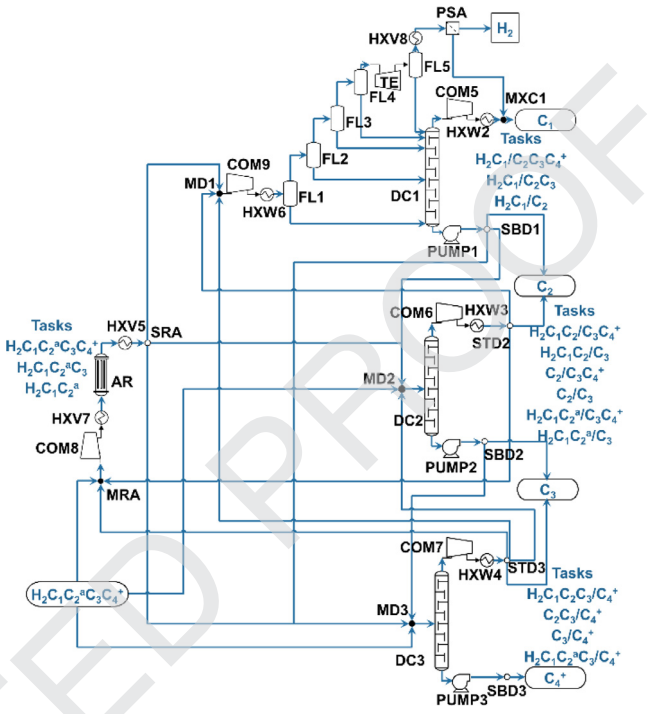

Fig. 2. State-equipment-network representation of the main separation train. H_2 (hydrogen), C_1 (methane); C_2 (ethane and ethylene); C_2^a (ethane, ethylene, and acetylene); C_3 (components with 3 carbon atoms), and C_4^+ (components with 4 or more carbon atoms).

In this work, the task assignment is based on the location of the separation cut for distillation columns (Novak et al., 1996; Yeomans and Grossmann, 1999b). While this approach is more complex in terms of column connectivity than the one proposed in the literature (Yeomans and Grossmann, 1999a), it has the potential to improve computational performance during the optimization procedure since it presents less variation in physical properties between discrete tasks (Mencarelli et al., 2020).

In the superstructure representation, we include units (u), which can correspond to process equipment units, raw materials, products or states, as shown in Fig. 2. The streams are defined by the connection between two different units. Thus, $F_{u1,u,j}$ and $x_{u1,u,j}$ are molar flowrate and molar fraction of component j for the process stream that leaves $u1$ and enters u, respectively. $T_{u1,u}$, $P_{u1,u}$, and $H_{u1,u}$ correspond to temperature, pressure and enthalpy flow of process streams that leave unit $u1$ and enter unit u. For the sake of simplicity, unit u output temperature is mapped into variable Tu_u, while Q_u and W_u are heat duty and work associated to unit u, respectively. The phase of a stream is predefined, except for streams related to states. Thus, the calculation of pure component enthalpy depends on its phase. $Hj_{p,u,j}$ is the specific enthalpy in phase p of component j evaluated at the process stream temperature that leaves unit u. In the same way, $xv_{u,j}$ and $xl_{u,j}$ are vapor and liquid stream molar fractions for component j leaving unit u of, respectively. Regarding the economics, CC_u is the capital cost associated to unit u.

States (Ust) are used to model discrete decisions regarding the separation system (see Fig. 2). Splitters and mixers with only one non-zero input and output stream are modeled with linear equations to eliminate nonconvex terms (Kocis and Grossmann, 1989). These units are considered to be states and referred to as SEN-mixers and SEN-splitters.

The three candidate columns to be the first one and the acetylene reactor are shown in Fig. 2, where the possible input and output states in each equipment unit are also shown. These states are defined by the presence of component groups, which are as follows: H_2 (hydrogen), C_1 (methane); C_2 (ethane and ethylene); C_2^a (ethane, ethylene, and acetylene); C_3 (components with 3 carbon atoms), and C_4^+ (components with 4 or more carbon atoms). As equipment unit interconnections shown in Fig. 2 are unknown beforehand, they are subject to discrete decisions and modeled as described in the next section. The acetylene hydrogenation reactor has also been modeled with a SEN approach. We only consider front-end configurations for the acetylene hydrogenation unit since this configuration is the most energy-efficient one (Zimmermann and Walzl, 2009). Consequently, H_2, C_1 and C_2^a species must be in the acetylene reactor feed stream.

Considering that each unit can only perform one task, Fig. 2 shows that each state has at most one non-zero input flow and output flow. Besides, considering that flowrate, temperature, pressure and enthalpy of non-existing streams are forced to be zero, state units include the following equations:

$$\sum_{u1\epsilon UI_u} T_{u1,u} = \sum_{u2\epsilon UO_u} T_{u,u2} \;\; u\epsilon Ust \tag{1.1}$$

$$\sum_{u1\epsilon UI_u} P_{u1,u} = \sum_{u2\epsilon UO_u} P_{u,u2} \;\; u\epsilon Ust \tag{1.2}$$

$$\sum_{u1\epsilon UI_u} H_{u1,u} = \sum_{u2\epsilon UO_u} H_{u,u2} \;\; u\epsilon Ust \tag{1.3}$$

where UI_u and UO_u are subsets of units that define the connection between units.

$$UI_u = \{u1 : u \; has \; input \;\; flowrate \;\; from \; u1\}$$

$$UO_u = \{u2 : u \; has \; output \;\; flowrate \; to \; u2\}$$

Regarding the disjunctions associated with the SEN representation, they include the state assignment based on task selection in equipment units. The corresponding formulation is as follows:

$$\mathrm{V}_{t\epsilon Ta_u}\begin{bmatrix} YT_{u,t} \\ \left.\begin{array}{l} F_{u1,u',j} = F_{u',u2,j} \\ T_{u1,u'} = T_{u',u2} \\ P_{u1,u'} = P_{u',u2} \\ H_{u1,u'} = H_{u',u2} \end{array}\right\} \begin{array}{c} j\epsilon J \\ u1\epsilon Us^{in}_{u',u,t} \\ u2\epsilon UO_{u'} \\ u'\epsilon Uis_u \end{array} \\ \left.\begin{array}{l} F_{u',u2,j} = F_{u1,u',j} \\ T_{u',u2} = T_{u1,u'} \\ P_{u',u2} = P_{u1,u'} \\ H_{u',u2} = H_{u1,u'} \end{array}\right\} \begin{array}{c} j\epsilon J \\ u1\epsilon UI_{u'} \\ u2\epsilon Us^{out}_{u,u',t} \\ u'\epsilon Uos_u \end{array} \end{bmatrix} u \in USEN \tag{2}$$

$$USEN = \{DC1, DC2, DC3, AR, DC7, DC8\}$$

where $Us^{in}_{u',u,t}$ is the state that is fed through SEN-mixer u' and processed in unit u when task t is selected; $Us^{out}_{u,u',t}$ is the state that is delivered through splitter u' and produced in unit u when task t is selected; Uis_u is the set of SEN-mixers that feed process unit u; Uos_u is the set of SEN-splitters that deliver an output stream from u. $YT_{u,t}$ and Ta_u are defined in Section 3.1.

Eqs. (3.1)-(3.5) are included to enforce the consistency of tasks in columns (Yeomans and Grossmann, 2000). Eqs. (3.1) and (3.4) ensure that the initial states are only fed to one unit, while constraints (3.2) and (3.3) allow only one source for states C_2 and C_3, respectively. Eq. (3.5) is an exclusive OR of the tasks performed in an equipment unit.

$$YT_{DC2,C_1C_2^a/C_3C_4} \veebar YT_{DC3,C_1C_2^aC_3/C_4} \veebar YT_{C2H,C_1C_2^aC_3C_4} \tag{3.1}$$

$$YT_{DC1,C_1/C_2} \veebar\veebar YT_{DC2,C_2/C_3C_4} \veebar YT_{DC2,C_2/C_3} \tag{3.2}$$

$$YT_{DC3,C_3/C_4} \veebar YT_{DC2,C_1C_2/C_3} \veebar YT_{DC2,C_2/C_3} \veebar YT_{DC2,C_1C_2^a/C_3} \tag{3.3}$$

$$YT_{DC7,C_2/C_3C_4} \veebar !YT_{DC8,C_2C_3/C_4} \tag{3.4}$$

$$\underline{\mathrm{V}}_{t\epsilon Ta_u} YT_{u,t} \;\; u\epsilon USEN \tag{3.5}$$

3.3. Logic-based outer approximations algorithm

The Logic-based Outer Approximation (L-bOA) algorithm is applied to solve the complex GDP model that exploits the logical structure to avoid "zero-flow" numerical difficulties that arise in nonlinear network design problems when nodes or streams disappear. In this work, we have carried out a custom implementation of L-bOA in GAMS, as it is no longer available in commercial software environments (LOGMIP). The L-bOA algorithm (Türkay and Grossmann, 1996, Vecchietti and Grossmann, 2000, Chen et al., 2018) proceeds by performing a set covering step in which selected Nonlinear Programming (NLPs) subproblems are solved for nonlinear disjunctions, whose solutions provide points to obtain linearizations for all nonlinear constraints involved in the disjunctions of the original GDP model. The lowest solution value of these NLP subproblems yields an upper bound to the problem (z1), in a minimization case. Thus, a linear GDP is generated, which is in turn reformulated (in our case) through a Big M reformulation as an MILP (including the Equation Relaxation-Augmented Penalty function, ER-AP, strategy). The solution of this MILP provides an estimate of the optimal topology. This information is transferred to the GDP problem in order to fix Boolean variables at the optimal topology and to solve a reduced NLP subproblem. If the objective function value z2 is greater than z1, the optimal solution is found (worsening of the objective function); otherwise, the upper bound to the problem is updated to z2, and new linearizations and integer cuts are added to the linear GDP and iterations continue until convergence.

4. Mathematical model

The proposed superstructure includes rigorous models for different types of reactors, heat exchangers, flash tanks, a turboexpander, compressors, pumps, mixers, splitters, distillation columns and states. The performance of each equipment unit model has been compared to Aspen Plus rigorous simulations of the corresponding unit, resulting in relative errors of less than 4 %. Equipment units are described in this section, except for the case of flash tanks and the turboexpander, whose models are described in the Supplementary Material. Furthermore, we develop correlations for pure component properties, for which the R^2 coefficients are higher than 0.99 in each case.

4.1. General equations

Material balance equations for process units are formulated as follows,

$$\sum_{u1\epsilon UI_u} F_{u1,u,j} = \sum_{u2\epsilon UO_u} F_{u,u2,j} \;\; j\epsilon J, \;\; u\epsilon U\backslash Uex \tag{4}$$

where U is the set of units, and Uex is the set of units excluded from this balance, which includes reactors, raw material, and products. UI_u and UO_u are defined in Section 3.2.

Pressure balances are written as follows,

$$P_{u1,u} \le P_{u,u2} \;\; u1\epsilon UI_u, u2\epsilon UO_u, u\epsilon U\backslash(Upc \cup Ust) \tag{5.1}$$

$$P_{u1,u} \ge P_{u,u2} \;\; u1\epsilon UI_u, \;\; u2\epsilon UO_u, u\epsilon\{Upc \cup Ust\} \tag{5.2}$$

where Upc is the set of pressure change units, which includes compressors and pumps, and Ust is the set of states. In particular cases, such as reactive furnaces and propane dehydrogenation reactors, a pressure drop in u is considered and denoted by DPu_u.

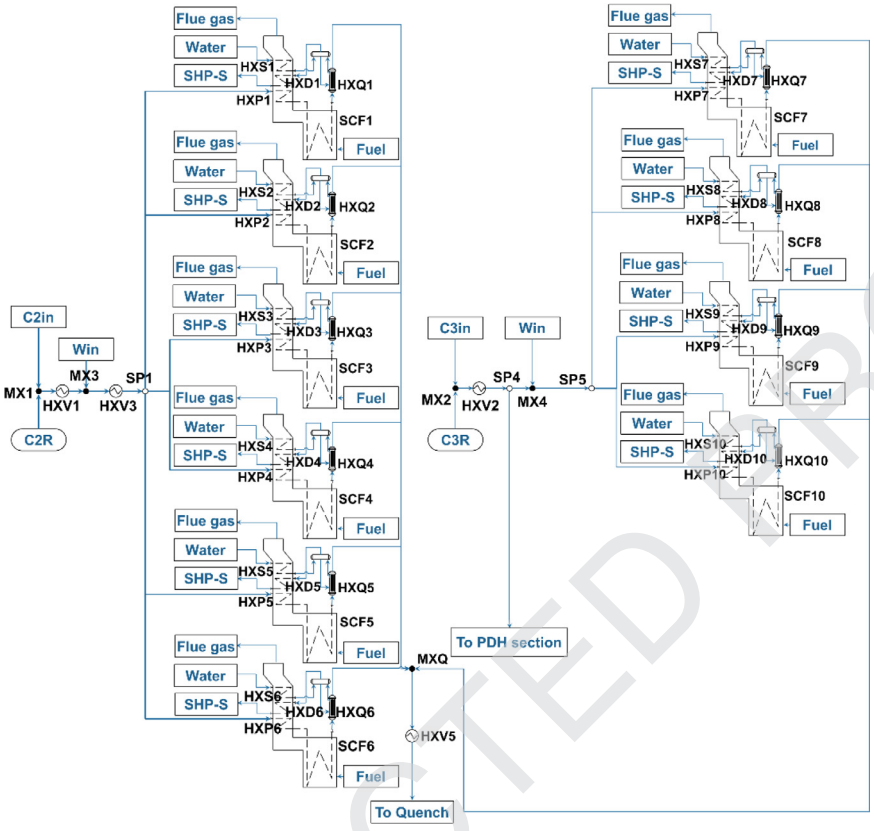

Fig. 3. Ethane and propane cracking furnaces. C2in (ethane). C3 (propane). C2R (Ethane recycle). SHP-S (super high-pressure steam).

Heat balances for reactors (Ur), heat exchangers (Uhx) and vessel units ($Uves$) are as follows

$$Q_u = \sum_{u2 \epsilon UO_u} H_{u,u2} - \sum_{u1 \epsilon UI_u} H_{u1,u} \quad u \epsilon \{Ur \cup Uhx \cup Uves\} \tag{6}$$

Vapor and liquid enthalpy of pure components are calculated with Eqs. (7.1) and (7.2), respectively, which are low order polynomial functions derived from DIPPR database (Wilding et al., 1998) for tighter temperature bounds associated to process conditions,

$$f_j^{VAP}(Tu_u) = H_j^0 + \sum_{i=1}^{4} \frac{cf_{CP,j,i}}{i} \left(Tu_u{}^i - Tref^i\right) \tag{7.1}$$

$$f_j^{LIQ}(Tu_u) = \sum_{i=1}^{5} cf_{HL,j,i} Tu_u{}^{i-1} \tag{7.2}$$

where $cf_{CP,j,i}$ and $cf_{HL,j,i}$ are parameters, and H_j^0 is the component enthalpy evaluated at the reference temperature $Tref$. Partial pressures of pure components are calculated with the extended Antoine equation (Green and Perry, 2007), as follows,

$$f_j^{pvap}(Tu_u) = cf_{AN,j,1} + \frac{cf_{AN,j,2}}{Tu_u} + cf_{AN,j,3} Log(Tu_u) + cf_{AN,j,4} Tu_u{}^{cf_{AN,j,5}} \tag{8}$$

where $cf_{AN,j,i}$ are component parameters.

Molar Liquid volume of pure components are calculated through a polynomial function based on DIPPR database (Wilding et al., 1998), as follows,

$$f_j^b(Tu_u) = \sum_{i=1}^{4} cf_{VL,j,i} \cdot Tu_u{}^{i-1} \tag{9}$$

4.2. Cracking furnaces

The cracking furnaces are modeled as a combination of units to consider the alkane steam cracking reaction inside coils, natural gas combustion outside the coils, feeding preheating, and the integration for the super high-pressure steam (SHP-steam).

Two reactive sections are identified in the furnace; the first one (Usc) describes the cracking reaction inside the coils, while the second one describes the combustion reaction outside the coils (Ucb_u). As both sections have gas outlet streams, they include equations to calculate outlet stream vapor enthalpy (Eq. (7.1)) and the duty (Eq. (6)). It should be noted that fuel combustion outside coils supplies heat to the cracking reaction, where there is one-to-one assignment between units in Ucb_u and Usc, and this constraint is represented in (10).

$$Q_u + Q_{u1} = 0 \quad u1 \epsilon Ucb_u, u \epsilon Usc \tag{10}$$

The cracking furnaces are modeled with disjunction (11), where Qf_u is the overall heat exchanged in the furnace; and $Ucbo_{u3}$ is the subset of units including the heat exchanger that provides heat from the flue gas in $u3$; $SCF1$ *to* $SCF6$ are ethane steam crackers and $SCF7$ *to* $SCF10$ are propane steam crackers (see Fig. 3). Regarding reactions within coils, the reactive furnaces can employ ethane or propane as raw material, thus, Jr_u is defined as the set that contains this reactive species in unit u. The cracking reactions are modeled with carbon yields ($CY_{u,j1,j}$), where the parameter $CY_{u,j1,j}$ is the carbon yield of component j from reactive component $j1$ in unit u, which is obtained from mass yields reported in the literature (Zimmermann and Walzl, 2009). Atom balances are also included, where the parameter $At_{j,a}$ is the number of atoms a in component j. Furthermore, the variables $Fi_{j1,j}$ and Hi_{j1} are auxiliary variables included to ensure that furnaces fed with the same raw material have the same feed flowrate. Complete combustion of fuel is assumed in furnaces with a 10% excess of air. Non-reactive steps in these units correspond to the heat exchanger network within the furnace, and are modeled through vapor phase heat exchangers, whose disjunctive models are presented in Section 4.7.

$$
\begin{bmatrix}
Y_u & \\
F_{u1,u,j1}At_{j1,C}CY_{u,j1,j} + At_{j,C}\left(F_{u1,u,j} - F_{u,u2,j}\right) = 0 \;\; j\epsilon J, j1\epsilon Jr_u & \text{Carbon yields} \\
\sum_{j\epsilon J} F_{u1,u,j}At_{j,a} = \sum_{j\epsilon J} F_{u,u2,j}At_{j,a} \quad a\epsilon AT & \text{Atom balances} \\
\left.\begin{array}{c} Hj_{VAP,u,j} = f_j^{VAP}\left(T_{u,u2}\right) \\ H_{u,u2} = \sum_{j\epsilon J} Hj_{VAP,u,j}F_{u,u2,j} \\ Tu_u = T_{u,u2} \end{array}\right\} & \text{Enthalpy eqns.} \\
P_{u,u2} = P_{u1,u} - DPu_u \quad \text{Pressure bal.} & \\
\left.\begin{array}{c} F_{u1,u,j} = Fi_{j1,j} \;\; j\epsilon J, j1\epsilon Jr_u \\ H_{u1,u} = Hi_{j1} \;\; j\epsilon J, j1\epsilon Jr_u \end{array}\right\} \text{Input split} & \\
\left.\begin{array}{c} \sum_{j\epsilon J} F_{u4,u3,j}At_{j,C} = F_{u3,u5,CO_2} \\ \sum_{j\epsilon J} F_{u4,u3,j}At_{j,H} = F_{u3,u5,H_2O} \\ \sum_{j\epsilon J} F_{u4,u3,j}At_{j,O} = \sum_{j\epsilon J} F_{u3,u5,j}At_{j,O} \\ F_{u4,u3,N_2} = F_{u3,u5,N_2} \\ 0.1\left(F_{u1,u,O_2} - F_{u,u2,O_2}\right) = F_{u,u2,O_2} \end{array}\right\} & \text{Atom balances in combustion box} \\
\left.\begin{array}{c} Hj_{VAP,u5,j} = f_j^{VAP}\left(Tu_{u3}\right) \\ H_{u3,u5} = \sum_{j\epsilon J} Hj_{VAP,u5,j}F_{u3,u5,j} \\ Tu_{u3} = T_{u3,u5} \end{array}\right\} & \text{Enthalpy eqns. of combustion box} \\
\left.\begin{array}{c} Qf_u = H_{u4,u3} - H_{u6,FlueGas} \;\; u6\epsilon Ucbo_{u3} \\ CC_u = g^f\left(Qf_u\right) \end{array}\right\} & \text{Capital cost}
\end{bmatrix}
\vee
\begin{bmatrix}
\neg Y_u \\
F_{u1,u,j} = 0 \\
F_{u,u2,j} = 0 \\
H_{u1,u} = 0 \\
H_{u,u2} = 0 \\
F_{u4,u3,j} = 0 \\
F_{u3,u5,j} = 0 \\
H_{u4,u3} = 0 \\
H_{u3,u5} = 0 \\
CC_u = 0
\end{bmatrix}
$$

$$
\begin{array}{l} u5\epsilon UO_{u3}, u4\epsilon UI_{u3}, u3\epsilon Ucb_u, u2\epsilon UO_u, u1\epsilon UI_u, u\epsilon Usc \\ Usc = \{SCF1, SCF2, SCF3, SCF4, SCF5, SCF6, SCF7, SCF8, SCF9, SCF10\} \end{array} \tag{11}
$$

As the cracking furnace section includes several units apart from the furnaces themselves (Fig. 3), the selection of one furnace implies the selection of the associated equipment units. Therefore, logical equations are included to take into account these constraints. For instance, the selection of the first furnace ($SCF1$), which operates with ethane feed, involves the selection of combustion box $CB1$, the feeding preheater $HXP1$, the steam overheater $HXD1$, the transfer line exchanger $HXQ1$, and the water preheater $HXS1$, whose existence is modeled through the following logical expressions:

$$Y_{SCF1} \Leftrightarrow Y_{CB1}; Y_{SCF1} \Leftrightarrow Y_{HXP1}; Y_{SCF1} \Leftrightarrow Y_{HXD1}; Y_{SCF1} \Leftrightarrow Y_{HXS1}; Y_{SCF1} \Leftrightarrow Y_{HXQ1} \tag{12}$$

Analogous equations are included for the rest of the steam cracking furnaces, and these logical relations are transformed into integer constraints according to the literature (Raman and Grossmann, 1991).

Furthermore, there are symmetric solutions since there is no difference between the furnaces that process the same alkane. For this reason, we include symmetry breaking Eqs. (13.1) and (13.2) for ethane and propane furnaces, respectively.

$$Y_{SCF2} \Rightarrow Y_{SCF1}; \;\; Y_{SCF3} \Rightarrow Y_{SCF2}; Y_{SCF4} \Rightarrow Y_{SCF5}; \;\; Y_{SCF5} \Rightarrow Y_{SCF6} \tag{13.1}$$

$$Y_{SCF7} \Rightarrow Y_{SCF8}; Y_{SCF8} \Rightarrow Y_{SCF9}; \;\; Y_{SCF9} \Rightarrow Y_{SCF10} \tag{13.2}$$

The selection of the first furnace to process ethane ($SCF1$) implies the presence of the units related to ethane feed, then the logic implications (14.1) are also included, which means the presence of the heat exchangers $HXV1$, $HXV3$, the mixers $MX1$ and $MX3$, and the splitter $SP1$. In the same way, the selection of the first furnace that processes propane ($SCF7$) involves logic equations shown in (14.2), which imply the presence of the mixer $MX4$ and the splitter $SP5$.

$$Y_{SCF1} \Leftrightarrow Y_{HXV1}; Y_{SCF1} \Leftrightarrow Y_{HXV3}; Y_{SCF1} \Leftrightarrow Y_{MX1}; Y_{SCF1} \Leftrightarrow Y_{MX3}; Y_{SCF1} \Leftrightarrow Y_{SP1} \tag{14.1}$$

$$Y_{SCF7} \Leftrightarrow Y_{MX4}; \;\; Y_{SCF7} \Leftrightarrow Y_{SP5} \tag{14.2}$$

The reactor size for ethylene production is a design variable since this olefin is required to satisfy market demand, but it could also be transformed into propylene in the plant. Thus, discrete decisions also appear in the number of furnaces to be included in this process.

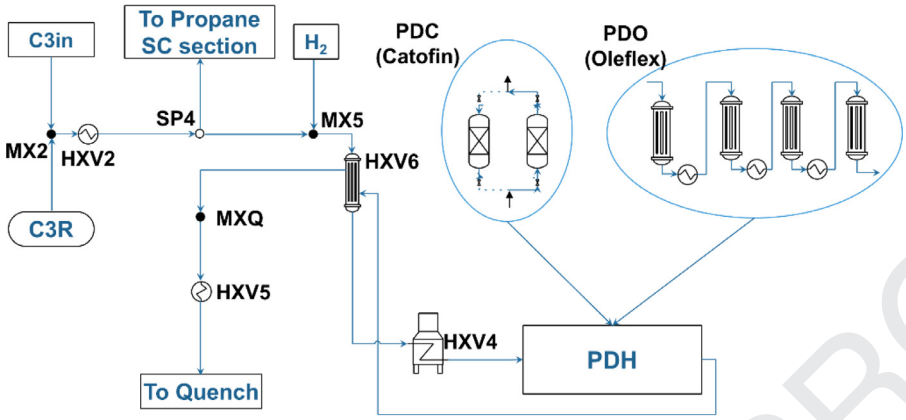

Fig. 4. Propane dehydrogenation alternatives (PDC and PDO).

4.3. Propane dehydrogenation reactors

Reactors for propane dehydrogenation are modeled applying carbon yields, which were obtained from the literature, (Chin et al., 2011) and (Węgrzyniak et al., 2017), for Oleflex and Catofin processes, respectively. It should be noted that in the case of including a propane dehydrogenation unit in the plant, only one technology can be selected, either the Pt-based or Cr-based process, as is shown in Fig. 4. In this case, we have embedded disjunctions. The first level decision is the selection of a propane hydrogenation unit, while the second level one is the specific technology selection, Oleflex or Catofin, which have different product selectivity and capital costs. Besides, the Oleflex process requires hydrogen co-feeding.

$$\left[\begin{array}{l} \left[\begin{array}{c} Y_{PDH} \\ Z_{PDC} \\ 3\,F_{u1,PDH,C_3H_8} CY_{PDC,C_3H_8,j} + \\ At_{j,C}\left(F_{u1,PDH,j} - F_{PDH,u2,j}\right) = 0\ j\epsilon J \\ F_{H2,MX5,H_2} = 0 \\ CC_{PDH} = g^{PDC}\left(F_{PDH,u2,C_3H_8}\right) \end{array}\right] \vee \left[\begin{array}{c} Y_{PDH} \\ Z_{PDO} \\ 3\,F_{u1,PDH,C_3H_8} CY_{PDO,C_3H_8,j} + \\ At_{j,C}\left(F_{u1,PDH,j} - F_{PDH,u2,j}\right) = 0\ j\epsilon J \\ F_{H2,MX5,H_2} = 0.82\,F_{SP4,MX5,C_3H_8} \\ CC_{PDH} = g^{PDO}\left(F_{PDH,u2,C_3H_8}\right) \end{array}\right] \quad \text{Carbon yields and capital cost} \\ \sum_{j\epsilon J} F_{u1,PDH,j} At_{j,a} = \sum_{j\epsilon J} F_{PDH,u2,j} At_{j,a} \quad a\epsilon AT \quad \text{Atom bal.} \\ \left.\begin{array}{c} Hj_{VAP,PDH,j} = f_j^{VAP}\left(T_{PDH,u2}\right) \\ H_{PDH,u2} = \sum_{j\epsilon J} Hj_{VAP,PDH,j} F_{PDH,u2,j} \\ Tu_{PDH} = T_{PDH,u2} \end{array}\right\} \quad \text{Enthalpy eqns.} \\ P_{PDH,u2} = P_{u1,PDH} - DPu_{PDH} \quad \text{Pressure balance} \\ u2\epsilon UO_{PDH}, u1\epsilon UI_{PDH} \end{array}\right] \vee \left[\begin{array}{c} \neg Y_{PDH} \\ F_{u1,PDH,j} = 0 \\ F_{PDH,u2,j} = 0 \\ H_{u1,PDH} = 0 \\ H_{PDH,u2} = 0 \\ CC_{PDH} = 0 \end{array}\right] \tag{15}$$

Logic relations derived from the nested disjunctions are as follows:

$$Z_{PDC} \veebar Z_{PDO};\ Z_{PDC} \vee Z_{PDO} \Leftrightarrow Y_{PDH};\ Y_{PDH} \Leftrightarrow Y_{MX5};\ Y_{PDH} \Leftrightarrow Y_{HXV4};\ Y_{PDH} \Leftrightarrow Y_{HXV6} \tag{16}$$

where Z_{PDC} and Z_{PDO} are Boolean variables associated with the selection of propane dehydrogenation through Catofin process and Oleflex process, respectively.

4.4. Hydrogenation reactors

4.4.1. Acetylene hydrogenation reactor

In the acetylene dehydrogenation reactor (AR), front-end hydrogenation is considered as it has numerous advantages over tail-end configuration (Zimmermann and Walzl, 2009). These include no hydrogen make-up, catalyst regeneration is less frequent, and light ends do not have to be removed in ethylene splitters, allowing operation at low pressure in this unit. As mentioned in Section 3.2, the reactor (AR) has been modeled with a SEN approach (see Fig. 2). A surrogate model is developed for this reactor with ALAMO (Cozad et al., 2014), based on a rigorous model (Mansoornejad et al., 2008). The surrogate model provides good agreement with data from the rigorous model, giving an R^2 coefficient higher than 0.99, which is considered accurate enough for this application. In this way, ethylene conversion ($XV_{C_2H_4}$) is calculated from (17.1). The relevant variables of this surrogate are the input molar fraction of acetylene (x_{HXV7,AR,C_2H_2}, calculated from Eq. (17.2)), and acetylene conversion ($XV_{C_2H_2}$, calculated from Eq. (17.3)). Furthermore, this unit includes atom balances for chemical species that are involved in reactions (17.4), material balances for inert species (17.5), and equations to calculate the output stream vapor enthalpy (17.6) and (17.7). Equation (17.8) is a connection equation, and the capital cost is estimated with Eq. (17.9).

$$XV_{C_2H_4} = f^{XE}\left(x_{HXV7,AR,C_2H_2}, XV_{C_2H_2}\right) \tag{17.1}$$

$$x_{u1,AR,C_2H_2} \sum_{j1\epsilon J} F_{u1,AR,j1} = F_{u1,AR,j}\ \ j\epsilon J,\ \ u1\epsilon UI_{AR} \tag{17.2}$$

$$F_{u1,AR,j}\left(1 - XV_j\right) = F_{AR,u2,j} \;\; u1\epsilon UI_{AR}, u2\epsilon UO_{AR}, \; j\epsilon\{C_2H_2, C_2H_4\} \tag{17.3}$$

$$\sum_{j\epsilon\{H_2,C_2H_2,C_2H_4,C_2H_6\}} \left(F_{u1,AR,j}At_{j,a} - F_{AR,u2,j}At_{j,a}\right) = 0 \;\; u1\epsilon UI_{AR}, u2\epsilon UO_{AR}, \;\; a\epsilon\{C, H\} \tag{17.4}$$

$$\sum_{u1\epsilon UI_{AR}} F_{u1,AR,j} = \sum_{u2\epsilon UO_{AR}} F_{AR,u2,j} \;\; j\epsilon J\backslash\{H_2, C_2H_2, C_2H_4, C_2H_6\} \tag{17.5}$$

$$Hj_{VAP,AR,j} = f_j^{VAP}(T_{AR,u2}) \;\; u2\epsilon UO_{AR} \tag{17.6}$$

$$H_{AR,u2} = \sum_{j\epsilon J} Hj_{VAP,AR,j}F_{AR,u2,j} \;\; u2\epsilon UO_{AR} \tag{17.7}$$

$$Tu_{AR} = T_{AR,u2} \;\; u2\epsilon UO_{AR} \tag{17.8}$$

$$CC_{AR} = g^{AR}\left(F_{u1,AR,C_2H_2}\right) \;\; u1\epsilon UI_{AR} \tag{17.9}$$

4.4.2. Methylacetylene and Propadiene (MAPD) hydrogenation reactor

The catalytic hydrogenation of C3 cut ($C3H$) is required to eliminate methylacetylene and propadiene (MAPD). A rigorous model based on the literature (Qian et al., 2015) is formulated to represent this unit. Numerical results obtained with this model show that the selectivity towards propylene is high enough to assume that there is full conversion from MAPD to the olefin (18.1) and its output flowrate is zero (18.2). On the other hand, Eq. (18.3) calculates hydrogen flowrate entering the unit ($H2C_u$), and Eq. (18.4) is a material balance for inert chemical species. Further, since the hydrogenation reaction takes place in liquid phase, it is assumed that the output stream is at its bubble point. To consider this equilibrium condition, Eqs. (18.5)-(18.11) are included, where $Lp_{u,j}$ is the logarithm of the vapor pressure, which is calculated from the extended Antoine equation (Green and Perry, 2007).

$$\sum_{u1\epsilon UI_u} \left(F_{u1,C3H,C_3H_4} + F_{u1,C3H,C_3H_6}\right) = \sum_{u2\epsilon UO_u} F_{C3H,u2,C_3H_6} \tag{18.1}$$

$$F_{C3H,u2,C_3H_4} = 0 \;\; u2\epsilon UO_{C3H} \tag{18.2}$$

$$H2C_{C3H} = F_{u1,C3H,C_3H_4} \;\; u1\epsilon UI_{C3H} \tag{18.3}$$

$$\sum_{u1\epsilon UI_u} F_{u1,C3H,j} = \sum_{u2\epsilon UO_u} F_{C3H,u2,j} \;\; j\epsilon J\backslash\{C_3H_4, C_3H_6\} \tag{18.4}$$

$$Hj_{LIQ,C3H,u2,j} = f_j^{LIQ}(Tu_{C3H}) \;\; j\epsilon J, u2\epsilon UO_{C3H} \tag{18.5}$$

$$H_{C3H,u2} = \sum_{j\epsilon J} Hj_{LIQ,C3H,j}F_{C3H,u2,j} \;\; u2\epsilon UO_{C3H} \tag{18.6}$$

$$Tu_{C3H} = T_{C3H,u2} \;\; u2\epsilon UO_{C3H} \tag{18.7}$$

$$Lp_{C3H,j} = f_j^{pvap}(Tu_u) \;\; j\epsilon J \tag{18.8}$$

$$xl_{C3H,j}\sum_{j1\epsilon J} F_{u1,C3H,j1} = F_{u1,C3H,j} \;\; j\epsilon J, u1\epsilon UI_{C3H} \tag{18.9}$$

$$\sum_{j\epsilon J} \exp(Lp_{C3H,j})xl_{C3H,j} = P_{C3H,u2} \;\; u2\epsilon UO_{C3H} \tag{18.10}$$

$$CC_{C3H} = g^{C3H}\left(F_{C3H,u2,j}\right) \;\; u2\epsilon UO_{C3H} \tag{18.11}$$

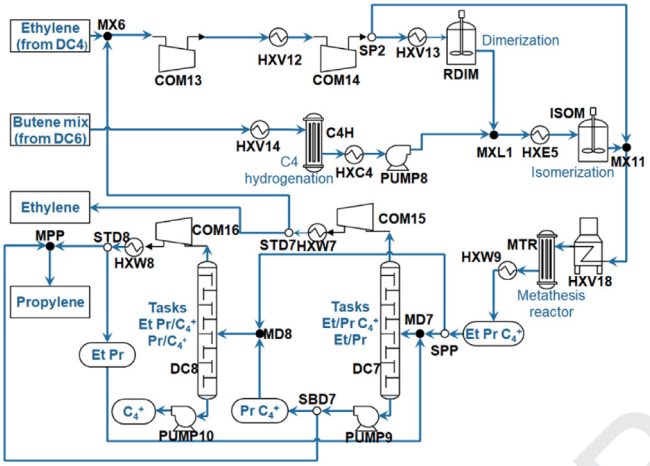

Fig. 5. Metathesis section.

4.5. Metathesis section model

In this section propylene is produced through ethylene and butenes metathesis (Mazoyer et al., 2013). The entire process is shown in Fig. 5 and includes a dimerization, C4 hydrogenation, isomerization and metathesis reactors, as well as two product purification columns. A detailed description of the corresponding mathematical models is given below.

4.5.1. Dimerization reactor

The dimerization reactor (*DIM*) model is formulated based on carbon yields of reactive species (*JDr*) reported in the literature (Forestière et al., 2009), and material balances for inert species. As this reactor operates at the mixture bubble point, its model includes equations similar to those included for the C3 cut hydrogenation. The following disjunction is included:

$$
\begin{bmatrix}
Y_u \\
\left(F_{u1,u,j} - F_{u,u2,j}\right) At_{j,C} + 2\, CY_{u,C_2H_4,j} F_{u1,u,C_2H_4} = 0 \;\; j \epsilon JDr \\
F_{u1,u,j} = F_{u,u2,j} \;\; j \epsilon J \setminus JDr \\
\left.\begin{aligned} Hj_{LIQ,u,j} &= f_j^{LIQ}(Tu_u) \;\; j \epsilon J \\ H_{u,u2} &= \sum_{j \epsilon J} Hj_{LIQ,u,j} F_{u,u2,j} \\ Tu_u &= T_{u,u2} \end{aligned}\right\} \\
\left.\begin{aligned} x_{u1,u,j} \sum_{j1 \epsilon J} F_{u1,u,j1} &= F_{u1,u,j} \;\; j \epsilon J \\ \sum_{j \epsilon J} \exp(Lp_{u,j})\, x_{u1,u,j} &= P_{u,u2} \\ Lp_{u,j} &= f_j^{pvap}(Tu_u) \end{aligned}\right\} \\
CC_u = g^{RDIM}\left(F_{u1,u,j}, Tu_u\right) \\
u2 \epsilon UO_u, u1 \epsilon UI_u, u \epsilon \{RDIM\} \\
JDr = \{C_2H_4, 1\text{-}C_4H_8, C_6H_{12}\}
\end{bmatrix}
\begin{array}{l}
\textit{Carbon yield} \\
\textit{Inert compound balances} \\
\\
\textit{Enthalpy eqns.} \\
\\
\\
\\
\\
\\
\textit{Bubble point eqns.} \\
\\
\\
\textit{Capital cost}
\end{array}
\quad \vee \begin{bmatrix} \neg Y_u \\ F_{u,u2,j} = 0 \\ Q_u = 0 \\ CC_u = 0 \end{bmatrix} \tag{19}
$$

There are logic constraints to account for a preheating step (*HXV*13), which will not be included if the metathesis reactor (*MTR*) is not selected in the plant:

$$Y_{RDIM} \Leftrightarrow Y_{HXV13}; Y_{RDIM} \Leftrightarrow Y_{MTR} \tag{20}$$

4.5.2. C4 hydrogenation reactor

The hydrogenation of the C4 cut (*C4H*) is modeled by using carbon yield reported in the literature (Koeppel et al., 1994). Total conversion of diene and enyne compounds (*JRb*) into butenes and oligomers (*JPb*) is assumed. The following disjunction is included to represent the C4 hydrogenation reactor:

$$\left[\begin{array}{c} Y_u \\ \left.\begin{array}{c}(F_{u1,u,j}-F_{u,u2,j})At_{j,C}+\sum_{j1\epsilon JRb}CY_{u,j1,j}F_{u1,u,j1}At_{j1,C}=0 \;\; j\epsilon JPb \\ F_{u,u2,j}=0 \;\; j\epsilon JRb \\ 2\,H2C_u=\sum_{j\epsilon J}At_{j,H}\left(F_{u,u2,j}-F_{u1,u,j}\right) \\ F_{u1,u,j}=F_{u,u2,j} \quad j\epsilon J\backslash\{JRb\cup JPb\} \\ Hj_{VAP,u,j}=f_j^{VAP}\left(T_{u,u2}\right)\;\; j\epsilon J \\ H_{u,u2}=\sum_{j\epsilon J}Hj_{VAP,u,j}F_{u,u2,j}\end{array}\right\} \text{Enthalpy eqns.} \\ CC_u=g^{C4H}\left(F_{u1,u,j}\right) \quad \text{Capital cost} \\ u2\epsilon UO_u, u1\epsilon UI_u, u\epsilon\{C4H\} \\ JRb=\{C_4H_4, C_4H_6\} \\ JPb=\{1\text{-}C_4H_8, cis\text{-}2\text{-}C_4H_8, C_6H_{12}\}\end{array}\right] \begin{array}{l}\text{Atom yield} \\ \vee\left[\begin{array}{c}\neg Y_u \\ F_{u,u2,j}=0 \\ H_{u,u2}=0 \\ CC_u=0\end{array}\right] \\ \text{Inert compounds eqns.}\end{array} \tag{21}$$

494 *4.5.3. Isomerization and metathesis reactors*

495 Reactors for isomerization (*ISO*) and metathesis (*MTR*) have similar modeling equations, and their reaction products are assumed to be
496 in equilibrium (Eqs. 22 and 23). Data from the literature (Jiang et al., 2016) are used to obtain correlations for the natural logarithm of
497 the equilibrium constant of reaction r in unit u ($KTeq_{u,r}$). In Eqs. (22) and (23), set r may contain reactions 1, 2 and/or 3. Reactions 1, 2
498 and 3 refer to isomerization of 1-butene to trans-2-butene, isomerization of cis-2-butene to trans-2-butene, and metathesis of ethylene
499 and trans-2-butene to propylene, respectively. It should be noted that reactions 1 and 2 occur in the isomerization reactor, while the three
500 reactions take place in the metathesis reactor. Since the number of moles remains constant in these reactions, the equilibrium constraints
501 are written as linear relations of $Ftl_{u,u2,j}$, which are logarithmic transformations of outlet flowrate for reactive species (*JIr* in isomerization
502 and *JMr* in metathesis reactor). In this way, the number of nonlinear terms in the model is reduced. Furthermore, in the case of metathesis,
503 selectivities towards higher alkenes are considered by using the parameters MTS_j, which were also taken from the literature (Jiang et al.,
504 2016).
Q2
505 In this way, disjunctions corresponding to isomerization and metathesis reactors are given by Eqs. (22) and (23), respectively.

$$\left[\begin{array}{c} Y_u \\ \left.\begin{array}{c}KTeq_{u,r}=f_r^k(Tu_u)\;\; r\epsilon\{1,2\} \\ KTeq_{u,1}=Ftl_{u,u2,trans\text{-}2\text{-}C_4H_8}-Ftl_{u,u2,1\text{-}C_4H_8} \\ KTeq_{u,2}=Ftl_{u,u2,trans\text{-}2\text{-}C_4H_8}-Ftl_{u,u2,cis\text{-}2\text{-}C_4H_8} \\ \exp(Ftl_{u,u2,j})=F_{u,u2,j}\;\; j\epsilon JIr\end{array}\right\} \text{Equilibrium eqs.} \\ \left.\begin{array}{c}\sum_{j\epsilon J}F_{u1,u,j}At_{j,a}=\sum_{j\epsilon J}F_{u,u2,j}At_{j,a}\;\; a\epsilon\{C,H\} \\ \sum_{j\epsilon J}F_{u1,u,j}=\sum_{j\epsilon J}F_{u,u2,j} \\ F_{u1,u,j}=F_{u,u2,j}\;\; j\epsilon J\backslash JIr\end{array}\right\} \vee\left[\begin{array}{c}\neg Y_u \\ F_{u,u2,j}=0 \\ H_{u,u2}=0 \\ CC_u=0\end{array}\right] u2\epsilon UO_u, u1\epsilon UI_u, u\epsilon\{ISO\} \\ \text{Atom, mole and inert compound balances} \\ \left.\begin{array}{c}Hj_{VAP,u,j}=f_j^{VAP}\left(T_{u,u2}\right) \\ H_{u,u2}=\sum_{j\epsilon J}Hj_{VAP,u,j}F_{u,u2,j} \\ Tu_u=T_{u,u2}\end{array}\right\} \text{Enthalpy eqns.} \\ CC_u=g^{ISO}\left(F_{u,u2,j}\right) \quad \text{Capital cost} \\ JIr=\{1\text{-}C_4H_8, trans\text{-}2\text{-}C_4H_8, cis\text{-}2\text{-}C_4H_8\}\end{array}\right] \tag{22}$$

$$\left[\begin{array}{c} Y_u \\ KTeq_{u,r} = f_r^k(Tu_u)\ r\epsilon\{1,2,3\} \\ KTeq_{u,1} = Ftl_{u,u2,trans\text{-}2\text{-}C_4H_8} - Ftl_{u,u2,1\text{-}C_4H_8} \\ KTeq_{u,2} = Ftl_{u,u2,trans\text{-}2\text{-}C_4H_8} - Ftl_{u,u2,cis\text{-}2\text{-}C_4H_8} \\ KTeq_{u,3} = 2Ftl_{u,u2,C_3H_6} - Ftl_{u,u2,C_2H_4} - Ftl_{u,u2,trans\text{-}2\text{-}C_4H_8} \\ \exp(Ftl_{u,u2,j}) = F_{u,u2,j}\ \ j\epsilon JMr\backslash\{C_5H_{10}, C_6H_{12}\} \\ \sum_{j\epsilon JMr} F_{u1,u,j}At_{j,a} = \sum_{j\epsilon JMr} F_{u,u2,j}At_{j,a}\ \ a\epsilon\{C,H\} \\ \sum_{j\epsilon J} F_{u1,u,j} = \sum_{j\epsilon J} F_{u,u2,j} \\ F_{u1,u,j} = F_{u,u2,j}\ \ j\epsilon J\backslash JMr \\ F_{u,u2,C_3H_6} - F_{u1,u,C_3H_6} + F_{u,u2,C_5H_{10}} + F_{u,u2,C_6H_{12}} = \frac{F_{u,u2,C_5H_{10}}}{MTS_{C_5H_{10}}} \\ F_{u,u2,C_3H_6} - F_{u1,u,C_3H_6} + F_{u,u2,C_5H_{10}} + F_{u,u2,C_6H_{12}} = \frac{F_{u,u2,C_6H_{12}}}{MTS_{C_6H_{12}}} \\ Hj_{VAP,u,j} = f_j^{VAP}(T_{u,u2}) \\ H_{u,u2} = \sum_{j\epsilon J} Hj_{VAP,u,j}F_{u,u2,j} \\ Tu_u = T_{u,u2} \\ CC_u = g^{MTR}(F_{u,u2,j}, Tu_u) \end{array}\right] \begin{array}{l} \text{Equilibrium eqs.} \\ \\ \\ \\ \\ \\ \text{Atom, mole and inert compounds balances} \\ \\ \\ \\ \\ \text{Byproducts} \\ \\ \\ \text{Enthalpy eqns.} \\ \\ \text{Capital cost} \end{array} \vee \left[\begin{array}{c} \neg Y_u \\ F_{u,u2,j} = 0 \\ H_{u,u2} = 0 \\ CC_u = 0 \end{array}\right]$$

$$u2\epsilon UO_u, u1\epsilon UI_u, u\epsilon\{MTR\}$$
$$JMr = \{C_2H_4, C_3H_6, 1\text{-}C_4H_8, trans\text{-}2\text{-}C_4H_8, cis\text{-}2\text{-}C_4H_8, C_5H_{10}, C_6H_{12}\} \quad (23)$$

The metathesis reactor is the core of the metathesis section. If this unit does not exist in the plant, the entire section will not be included. For such reason, the following logic equation is included:

$$Y_{MTR} \Leftrightarrow Y_u\ u\epsilon Umt$$
$$Umt = \{MX6, SP2, HXV14, C4H, HXC4, MXL1, HXE5, ISOM, MX11, HXV18, HXW9, DC7, DC8, SP3\} \quad (24)$$

where $MX6$ and $MX11$ are vapor mixers, $SP2$ and $SP3$ are splitters, $HXV14$, $HXV18$ and $HXW9$ are vapor phase heat exchangers, $HXC4$ is a condensing heat exchanger, $HXE5$ is an evaporative heat exchanger, $C4H$ is the C4 cut hydrogenation reactor, $ISOM$ is the isomerization reactor, $DC7$ and $DC8$ are the deethylenizer and depropylenizer, respectively.

4.6. Heat exchangers

Three types of heat exchangers are considered. The first one operates without phase change for vapor ($Uhxv$) and liquid ($Uhxl$) streams. The phase is predefined, and the calculation of output enthalpy is carried out using Eqs. (7.1) or (7.2) as appropriate. The existence of this type of heat exchanger is modeled with the disjunction shown in Eq. (25).

$$\left[\begin{array}{c} Y_u \\ Hj_{p,u,j} = f_j^p(Tu_u)\ \ j\epsilon J \\ H_{u,u2} = \sum_{j\epsilon J} Hj_{p,u,j}F_{u,u2,j} \\ Tu_u = T_{u,u2} \end{array}\right] \vee \left[\begin{array}{c} \neg Y_u \\ Q_u = 0 \\ T_{u1,u} = T_{u,u2} \end{array}\right] u1\epsilon UI_u, u2\epsilon UO_u, p\epsilon P_u, u\epsilon\{Uhxv \cup Uhxl\} \quad (25)$$

Two types of heat exchangers are included considering phase change. The first one ($Uhxc$) has a vapor input stream and produces a liquid at its bubble point (condensation). The other one ($Uhxe$) produces a vapor stream at its dew point from a liquid (evaporation). The index p indicates the phase (vapor or liquid) of the output stream, and the index m refers to the physical change, condensation (CON) or evaporation (EVA). These units are modeled through disjunction (26.1). Eqs. (26.2) and (26.3) are employed for the condensation and evaporation heat exchangers, respectively.

$$\left[\begin{array}{l} Y_u \\ Hj_{p,u,j} = f_j^p(Tu_u)\ \ j \in J \\ H_{u,u2} = \sum_{j\epsilon J} Hj_{p,u,j}F_{u,u2,j} \\ Tu_u = T_{u,u2} \\ Lp_{u,j} = f_j^{pvap}(Tu_u)\ \ j \in J \\ x_{u,u2,j} \sum_{j1\epsilon J} F_{u,u2,j1} = F_{u,u2,j}\ \ j \in J \\ P_{u,u2} = f^m(Lp_{u,j}, x_{u,u2,j}\ \ j\epsilon J) \end{array}\right] \vee \left[\begin{array}{l} \neg Y_u \\ Q_u = 0 \\ T_{u1,u} = T_{u,u2} \end{array}\right] u2 \in UO_u, p \in P_u, m \in M_u, u \in \{Uhxc \cup Uhxe\} \quad (26.1)$$

$$f^{CON}\left(Lp_{u,j}, x_{u,u2,j}\ j\epsilon J\right) = \sum_{j\epsilon J} \exp(Lp_{u,j}) x_{u,u2,j} \tag{26.2}$$

$$f^{EVA}\left(Lp_{u,j}, x_{u,u2,j}\right) = 1/\sum_{j\epsilon J} \exp(-Lp_{u,j}) x_{u,u2,j} \tag{26.3}$$

In the case of heat exchangers operating without phase change for vapor streams ($Uhxw$), we include an additional constraint to ensure that operating pressure is lower than the mixture dew pressure. This is particularly useful for cryogenic processes, where several vapor streams are chilled to temperatures close to their dew points, or even partial condensation (Rodríguez and Diaz, 2007). The corresponding disjunction is shown in Eq. (27).

$$\begin{bmatrix} Y_u \\ Hj_{VAP,u,j} = f_j^{VAP}(Tu_u)\ \ j \in J \\ H_{u,u2} = \sum_{j \in J} Hj_{VAP,u,j} F_{u,u2,j} \\ Tu_u = T_{u,u2} \\ Lp_{u,j} = f_j^{pvap}(Tu_u)\ \ j \in J \\ x_{u1,u,j} \sum_{j1 \in J} F_{u1,u,j1} = F_{u1,u,j}\ \ j \in J \\ f^{EVA}\left(Lp_{u,j}, x_{u1,u,j}\right) \geq P_{u,u2} \end{bmatrix} \vee \begin{bmatrix} \neg Y_u \\ Q_u = 0 \\ T_{u1,u} = T_{u,u2} \end{bmatrix} u1 \in UI_u, u2 \in UO_u, u \in Uhxw \tag{27}$$

4.7. Utilities

Most of the reactors, heat exchangers and vessels employ utilities to satisfy their energy requirements. In these cases, disjunctions (28) and (29) are employed to calculate the associated costs of cooling and heating utilities, respectively. Correlations f^{cu} and f^{hu} are based on the literature (Ulrich and Vasudevan, 2006).

$$\begin{bmatrix} Y_u \\ Tu_u - Tut_u \geq \Delta t_m \\ CcUt_u = f^{cu}(Tu_u, Q_u) \end{bmatrix} \vee \begin{bmatrix} \neg Y_u \\ CcUt_u = 0 \end{bmatrix} u\epsilon Ucu \tag{28}$$

$$\begin{bmatrix} Y_u \\ -Tu_u + Tut_u \geq \Delta t_m \\ ChUt_u = f^{hu}(Tu_u, Q_u) \end{bmatrix} \vee \begin{bmatrix} \neg Y_u \\ ChUt_u = 0 \end{bmatrix} u\epsilon Uhu \tag{29}$$

where Δt_m is the minimum temperature approach; Tut_u is the utility temperature; $CcUt_u$ and $ChUt_u$ are the cost of cooling and heating utilities, respectively; Ucu and Uhu are the subsets of units that require cooling and heating utilities, respectively.

Furthermore, where process streams are integrated, Eq. (30) is included

$$Q_u + Q_{u1} = 0\ \ (u, u1)\epsilon Uqm \tag{30}$$

where Uqm is the set of pairs of units that exchange heat.

4.8. Compressors

Centrifugal compressor physical behavior is modeled following Smith and van Ness (Smith and Van Ness, 1987). Compressors ($Ucomp$) include Eq. (31) as an overall energy balance. Disjunction (32) models the compressors behavior. “Enthalpy eqs.” calculate outlet vapor stream enthalpy. “Specific heat eqs.” define an average temperature ($Tcom_u$) for the compressor to calculate the average specific heat of the mixture (Cpm_u). “Power calculation” equations define the pressure ratio (PR_u) and the gas constant-average specific heat ratio (eg_u) to calculate the the compressor power (W_u). Finally, the correlation g^c estimates the capital cost associated with the compressor.

$$-W_u = \sum_{u2\epsilon UO_u} H_{u,u2} - \sum_{u1\epsilon UI_u} H_{u1,u}\ \ u\epsilon Ucomp \tag{31}$$

$$\begin{bmatrix} Y_u \\ \left.\begin{matrix} Hj_{VAP,u,j} = f_j^{VAP}(Tu_u)\ \ j\epsilon J \\ H_{u,u2} = \sum_{j\epsilon J} Hj_{VAP,u,j} F_{u,u2,j} \end{matrix}\right\} \text{Enthalpy eqs.} \\ \left.\begin{matrix} 2\,Tcom_u = T_{u1,u} + T_{u1,u} {PR_u}^{eg_u} \\ Cp_{u,j} = f_j^c(Tcom_u)\ j\epsilon J \\ Cpm_u \sum_{j\epsilon J} F_{u1,u,j} = \sum_{j\epsilon J} Cp_{u,j} F_{u1,u,j} \end{matrix}\right\} \text{Specific heat eqs.} \\ \left.\begin{matrix} P_{u,u2} = P_{u1,u} PR_u \\ {eg_u}^{-1} = \frac{10\,Cpm_u}{R} \\ W_u = -\sum_{j\epsilon J} F_{u1,u,j} \frac{Cpm_u T_{u1,u}}{\eta_u} \left({PR_u}^{eg_u} - 1\right) \end{matrix}\right\} \text{Power calculation} \\ CC_u = g^c(W_u)\ \ \text{Capital cost estimation} \end{bmatrix} \vee \begin{bmatrix} \neg Y_u \\ W_u = 0 \\ CC_u = 0 \\ P_{u,u2} = P_{u1,u} \\ T_{u,u2} = T_{u1,u} \end{bmatrix} u1\epsilon UI_u, u2\epsilon UO_u, u\epsilon Ucomp \tag{32}$$

where R is the gas constant; η_u is the isentropic efficiency of unit u; W_u is unit u power; Cpm_u is average specific heat; $Tcom_u$ is average outlet stream temperature in unit u; $Cp_{u,j}$ is the specific heat of component j; PR_u is the pressure ratio (P_{out}/P_{in}=$P_{u,u2}/P_{u1,u}$).

4.9. Pumps

The energy balance in pumps ($Upump$) is shown in Eq. (33.1). Temperature increase in these units is considered negligible, Eq. (33.2). The disjunction representing this unit is shown in Eq. (34).

$$-W_u = \sum_{u2 \epsilon UO_u} H_{u,u2} - \sum_{u1 \epsilon UI_u} H_{u1,u} \; u \epsilon Upump \tag{33.1}$$

$$T_{u,u2} = T_{u1,u} \tag{33.2}$$

$$\begin{bmatrix} Y_u \\ -W_u = 0.1\, Vl_u \frac{(P_{u,u2}-P_{u1,u})}{\eta_u} \\ Vl_u = \sum_{j \in J} F_{u,u1,j} Vlj_{u,j} \\ Vlj_{u,j} = f_j^b(Tu_u) \;\; j \in J \\ CC_u = g^{pump}(W_u) \end{bmatrix} \vee \begin{bmatrix} \neg Y_u \\ W_u = 0 \\ CC_u = 0 \\ P_{u,u2} = P_{u1,u} \end{bmatrix} u1 \in UI_u, u2 \in UO_u, u \in Upump \tag{34}$$

4.10. Mixers and splitters

Two types of mixers are considered due to predefined phases. All mixers include the heat balance shown in (35). Mixer units (Umx) are modeled with disjunction (36), where the output enthalpy is calculated depending on the phase type of the mixture.

$$\sum_{u1 \epsilon UI_u} H_{u1,u} = \sum_{u2 \epsilon UO_u} H_{u,u2} \tag{35}$$

$$\begin{bmatrix} Y_u \\ Hj_{p,u,j} = f_j^p(T_{u,u2}) \;\; j \epsilon J \\ H_{u,u2} = \sum_{j \epsilon J} Hj_{p,u,j} F_{u,u2,j} \end{bmatrix} \vee \begin{bmatrix} \neg Y_u \\ F_{u,u2,j} = 0 \\ H_{u,u2} = T_{u,u2} \end{bmatrix} u2 \epsilon UO_u, p \epsilon P_u, u \epsilon Umx \tag{36}$$

Splitter units (Usp) are modeled by the following disjunctions

$$\begin{bmatrix} Y_u \\ F_{u1,u,j} Rsp_{u,u2} = F_{u,u2,j} \;\; j \epsilon J \\ H_{u1,u} Rsp_{u,u2} = H_{u,u2} \\ \sum_{u2 \epsilon UO_u} Rsp_{u,u2} = 1 \\ T_{u1,u} = T_{u,u2} \\ P_{u1,u} = P_{u,u2} \end{bmatrix} \vee \begin{bmatrix} \neg Y_u \\ F_{u,u2,j} = 0 \;\; j \epsilon J \\ H_{u,u2} = 0 \end{bmatrix} u1 \epsilon UI_u, u2 \epsilon UO_u, u \epsilon Usp \tag{37}$$

where $Rsp_{u,u2}$ is the split fraction of stream that goes from u to $u2$.

In the superstructure, we also have disjunctive splitters (Uds), which can only have one output stream. In order to replace nonlinear equations for linear ones, disjunction (38) is used in such cases.

$$\vee_{u2 \epsilon UO_u} \begin{bmatrix} Y_{u2} \\ F_{u1,u,j} = F_{u,u2,j} \;\; j \in J \\ T_{u1,u} = T_{u,u2} \\ P_{u1,u} = P_{u,u2} \\ H_{u1,u} = H_{u,u2} \end{bmatrix} u1 \in UI_u, u \in Uds \tag{38}$$

4.11. Distillation columns

Distillation column units (Udc) are modeled with a rigorous approach (Biegler et al., 1997; Viswanathan and Grossmann, 1993), and are represented by disjunction (39). "Feed specifications" assign input flowrates ($DF_{u1,u,n,j}$) and enthalpy ($DH_{u1,u,n}$) to the separation stages in trays n (NS_u), being the column number of stages a parameter, NFe_u contains pairs $(u1, n)$ such that the stream from unit $u1$ to column u enters in stage n. In this paper, we formulate material balances based on component flowrate to reduce the number of nonlinear matrix entries in the model. Thus, material balances include component flowrate in the liquid phase ($Dfl_{u,n,j}$) and in the vapor phase ($Dfv_{u,n,j}$) at stage n. The corresponding material balances for condenser (CD_u) and reboiler (RB_u) are also included.

"Equilibrium eqs." calculate the liquid ($DL_{u,n}$)-to-vapor ($DV_{u,n}$) ratio ($DR_{u,n}$) in unit u at stage n, and stands for the criterion of equality of fugacities based on stage temperature ($DCt_{u,n}$) and pressure ($DCp_{u,n}$) and considering ideal thermodynamic behavior of the mixture, i.e., ideal gas law for the vapor phase and Raoult's law for the liquid phase, where the natural logarithm of partial pressure ($DLp_{u,n,j}$) is given by the extended Antoine equation (Eq. (8)) (Green and Perry, 2007). Vapor and liquid fractions of component j are calculated as $Dfv_{u,n,j} DR_{u,n}/DL_{u,n}$ and $Dfl_{u,n,j} DR_{u,n} DV_{u,n}$, respectively, since $DR_{u,n}$ is the liquid-to-vapor ratio at stage n. This formulation of the equilibrium condition reduces nonlinear matrix entries in the model and avoids introducing physical properties with high variability, which are difficult to scale (e.g. partial pressures are logarithmically scaled). The summation equations for liquid and vapor flowrates are included in the model.

Regarding enthalpy balances in separation stages, Qc_u and Qh_u correspond to the condenser and reboiler duties, respectively. Ideal mixture is considered to estimate the overall enthalpies of liquid ($Dhl_{u,n}$) and vapor ($Dhv_{u,n}$). A linear pressure profile is forced through "Pressure constraints". "Properties calculations" are functions to calculate pure component enthalpy (vapor and liquid phases) and partial pressure (logarithmically scaled). "Temp. profile constraints" impose temperature increase as stage n increases to ensure an appropriate temperature profile in the Master MILP problems. While this equation may be redundant in the NLP subproblems, it is not the case in the Master MILP problems. Connection equations for top and bottom streams variables are considered. "Utilities calculation" equations estimate the utility cost in the condenser and the reboiler. Finally, the capital cost associated with the distillation column u is estimated through function g^{DC}.

$$
\left[\begin{array}{rl}
Y_u & \\
F_{u1,u,j} = DF_{u1,u,n,j} & j\epsilon J, (u1,n)\epsilon NFe_u \\
H_{u1,u} = DH_{u1,u,n} & (u1,n)\epsilon NFe_u \\
\sum_{(u1,n)\epsilon NFe_u} DF_{u1,u,n,j} + Dfl_{u,n-1,j} + Dfv_{u,n+1,j} = & \\
Dfl_{u,n,j} + Dfv_{u,n,j} & j\epsilon J, n\epsilon NS_u \\
Dfv_{u,n+1,j} = Dfl_{u,n,j} + Dfv_{u,n,j} & j\epsilon J, n\epsilon CD_u \\
Dfl_{u,n-1,j} = Dfl_{u,n,j} + Dfv_{u,n,j} & j\epsilon J, n\epsilon RB_u \\
DL_{u,n} = DV_{u,n} DR_{u,n} & n\epsilon\{NS_u \cup CD_u \cup RB_u\} \\
Dfv_{u,n,j} DR_{u,n} DCp_{u,n} = & \\
Dfl_{u,n,j} \exp(DLp_{u,n,j}) & j\epsilon J, n\epsilon\{NS_u \cup CD_u \cup RB_u\} \\
\sum_{j\epsilon J} Dfv_{u,n,j} = DV_{u,n} & n\epsilon\{NS_u \cup CD_u \cup RB_u\} \\
\sum_{j\epsilon J} Dfl_{u,n,j} = DL_{u,n} & n\epsilon\{NS_u \cup CD_u \cup RB_u\} \\
\sum_{(u1,n)\epsilon NFe_u} DH_{u1,u,n} + Dhl_{u,n-1} + Dhv_{u,n+1} = & \\
Dhl_{u,n} + Dhv_{u,n} & j\epsilon J, n\epsilon NS_u \\
Dhv_{u,n+1} - Qc_u = Dhl_{u,n} + Dhv_{u,n} & j\epsilon J, n\epsilon CD_u \\
Dhl_{u,n-1} + Qh_u = Dhl_{u,n} + Dhv_{u,n} & j\epsilon J, n\epsilon RB_u \\
Dhv_{u,n} = \sum_{j\epsilon J} Dhvc_{u,n,j} Dfv_{u,n,j} & n\epsilon\{NS_u \cup CD_u \cup RB_u\} \\
Dhl_{u,n} = \sum_{j\epsilon J} Dhlc_{u,n,j} Dfl_{u,n,j} & n\epsilon\{NS_u \cup CD_u \cup RB_u\} \\
DCp_{u,n-1} - 2\,DCp_{u,n} + DCp_{u,n+1} = 0 & j\epsilon J, n\epsilon NS_u \\
P_{u,u1} \le P_{u,u2} & u1\epsilon UV_u, u2\epsilon UL_u \\
Dhvc_{u,n,j} = f_j^{VAP}(DCt_{u,n}) & j\epsilon J, n\epsilon\{NS_u \cup CD_u \cup RB_u\} \\
Dhlc_{u,n,j} = f_j^{LIQ}(DCt_{u,n}) & j\epsilon J, n\epsilon\{NS_u \cup CD_u \cup RB_u\} \\
DLp_{u,n,j} = f_j^{pvap}(DCt_{u,n}) & j\epsilon J, n\epsilon\{NS_u \cup CD_u \cup RB_u\} \\
DCt_{u,n} \le DCt_{u,n-1} & n\epsilon NS_u \\
Dfv_{u,n,j} = F_{u,u2,j} & j\epsilon J, n\epsilon CD_u, u2\epsilon UV_u \\
Dhv_{u,n} = H_{u,u2} & n\epsilon CD_u, u2\epsilon UV_u \\
DCt_{u,n} = T_{u,u2} & n\epsilon CD_u, u2\epsilon UV_u \\
DCp_{u,n} = P_{u,u2} & n\epsilon CD_u, u2\epsilon UV_u \\
Dfl_{u,n,j} = F_{u,u2,j} & j\epsilon J, n\epsilon RB_u, u2\epsilon UL_u \\
Dhl_{u,n} = H_{u,u2} & n\epsilon RB_u, u2\epsilon UL_u \\
DCt_{u,n} = T_{u,u2} & n\epsilon RB_u, u2\epsilon UL_u \\
DCp_{u,n} = P_{u,u2} & n\epsilon CD_u, u2\epsilon UV_u \\
CcUt_u = f^{cu}(DCt_{u,n}, Qc_u) & n\epsilon CD_u \\
ChUt_u = f^{hu}(DCt_{u,n}, Qh_u) & n\epsilon RB_u \\
CC_u = g^{DC}(Dfl_{u,n,j}, Dfv_{u,n,j}, DCp_{u,n}, DCt_{u,n}) &
\end{array}\right]
\begin{array}{l}
\\ \\ \text{Feed specifications} \\ \\ \\ \\ \text{Material balances} \\ \\ \\ \text{Equilibrium eqs.} \\ \\ \text{Summation eqs.} \\ \\ \\ \\ \\ \\ \\ \text{Enthalpy balances} \\ \\ \\ \\ \\ \\ \\ \text{Pressure constraints} \\ \text{Properties calculations} \\ \\ \text{Temp. profile constraint} \\ \\ \\ \\ \text{Top stream connection eqs} \\ \\ \\ \\ \text{Bottom stream connection eqs} \\ \\ \\ \text{Utilities calculation} \\ \\ \text{Capital cost estimation}
\end{array}
\vee \left[\begin{array}{c} \neg Y_u \\ F_{u,u2,j} = 0 \;\; j\epsilon J, u2\epsilon UO_u \\ H_{u,u2} = 0 \;\; u2\epsilon UO_u \end{array}\right] u\epsilon Udc \tag{39}
$$

4.12. Net present value calculation

The revenues for selling products, raw material costs and electricity cost are calculated as follows,

$$Rev_u = Price_u HPY \sum_{u1\epsilon UI_u, j\epsilon J} MW_j F_{u1,u,j} \;\; u\epsilon Upd \tag{40.1}$$

$$CRM_u = Price_u HPY \sum_{u1\epsilon UI_u, j\epsilon J} MW_j F_{u1,u,j} \;\; u\epsilon Urm \tag{40.2}$$

$$ElecT = \left(-W_{TE} - \sum_{u\epsilon Comp} W_u - \sum_{u\epsilon Pump} W_u\right) PriceE \cdot HPY \tag{40.3}$$

where MW_j is the molecular weight of component j; and $Price_u$ corresponds to either product price or raw material cost associated to unit u; and $PriceE$ is the electricity cost. Rev_u and CRM_u are annual revenues and costs associated to unit u, respectively; and $ElecT$ is electricity annual cost.

The investment cost ($CInv$) and the total income (TIn) are calculated as follows

$$CInv = \beta\varphi \sum_{u\epsilon CCU} CC_u \tag{41.1}$$

$$TIn = \left(\sum_{u\epsilon Prod} Rev_u - \sum_{u\epsilon Prod} CRM_u - \sum_{u\epsilon UT} (CcUt_u + ChUt_u) - ElecT - \gamma\ CInv \right)(1 - tax) \tag{41.2}$$

where β is the contingency and fee factor ($\beta = 1.3$); φ is the auxiliary facilities factor ($\varphi = 1.55$); tax is the net benefits tax ($tax = 0.35$); and γ is the maintenance cost fraction ($\gamma = 0.045$). CCU is the set of units that could require an investment included in the flowsheet.

The objective function is to maximize the net present value (NPV), which is calculated as follows:

$$NPV = -CInv(1 + \omega) + \frac{TIn}{\alpha} \tag{42.1}$$

$$\alpha = \frac{\theta(1+\theta)^{\tau}}{(1+\theta)^{\tau} - 1} \tag{42.2}$$

where ω is the working capital cost fraction (ω=0.1), and α is the annuity that is calculated for an interest rate (θ) of 15 % and a total project life (τ) of 15 years.

5. Results

5.1. Case study

In this work, we consider a given plant capacity of 500,000 t/y of ethylene and 500,000 t/y of propylene. We analyze different price scenarios for different countries: USA, European Union, Russia and Argentina. This last country is included due to its encouraging perspective in shale gas proven reserves (Delpino and Diaz, 2014; U.S. Energy Information Administration, 2013). We obtain the optimal scheme for each case. Price data were obtained from the literature (Boulamanti and Moya, 2017), except for the case of Argentina. For this last country, price data of ethane, propane, and pyrolysis gas were taken from a report available in the internet (Cohen, 2019); electricity price, from a webpage (GlobalPetrolPrices.com, 2019); and natural gas, from (Charles, 2019). Due to the lack of data for hydrogen price in Argentina, we assume it by considering that the ratio between hydrogen and methane price for the other countries ranges between 2.4 and 4.1 (Table 1) and selecting a value of 3.2 for Argentina. In this way a value of 500 EUR/t is obtained. Ethylene and propylene prices are considered to be global ones, which are reported in the literature (Boulamanti and Moya, 2017). It is worth noting the important differences in raw material costs in the different scenarios; e.g., USA prices for ethane and propane are 146 and 394 EUR/t, respectively, while in the European Union they are 612 EUR/t each. Raw material and utility costs, as well as product prices are shown in Table 1.

As previously mentioned, the L-bOA algorithm begins by carrying out a set covering step in which selected sub NLPs are solved, whose solutions provide points to obtain linearizations for all nonlinear constraints in the disjunctions in the model. In this particular case, special efforts were devoted to the initialization of rigorous model of process units. Considering these initializations and the special formulation of the superstructure under study, only one NLP subproblem includes all nonlinear equations. In this way, linearization of all nonlinear equations could be generated for the first Master MILP problem by solving one initial NLP subproblem, whose scheme is shown in Table 2. It must be pointed out that this initial NLP includes all steam cracking furnaces (for both ethane and propane), propane dehydrogenation, and metathesis section. Furthermore, the separation scheme of the first NLP problem is a demethanizer-first scheme, and the corresponding tasks are shown in Table 2. It is worth mentioning that for each price scenario, we obtain the same optimal configuration starting from different initial points. Although we cannot guarantee global optimality with our implementation of the L-bOA algorithm, the multi-start procedure allows finding high quality local solutions.

Table 1
Prices scenarios.

	Units	USA	EU	Russia	Arg
Natural gas	EUR/t	149	443	114	157
Ethane	EUR/t	146	612	297	350
Propane	EUR/t	394	612	550	295
Hydrogen	EUR/t	367	1344	466	500
Pygas	EUR/t	774	789	679	395
Electricity	EUR/MWh	35	85	39	56
Ethylene	EUR/t	973	973	973	973
Propylene	EUR/t	1030	1030	1030	1030

5.3. Model statistics

The GDP model is implemented in GAMS 24.2.3 (Rosenthal, 2014) and run on an Intel(R) Core(TM) i7–4790 CPU @3.60GHz and 8 GB RAM. As explained above, the entire problem is decomposed into reduced NLP and Master MILP problems, which are solved with CONOPT (Drud, 1994) and Cplex (IBM Corp. and IBM, 2009), respectively. The corresponding model statistics are shown in Table 3 for the USA price scenario.

Table 4 shows the most important discrete decisions that were determined for the four price scenarios. It can be seen that the optimal technology for USA and Russia price scenarios is the same, including four ethane steam cracking furnaces and olefin metathesis. Propane is not used as raw material, as its price is almost twice ethane price in both scenarios. Therefore, additional ethylene is produced by steam cracking and converted to propylene through ethylene dimerization and metathesis processes. Regarding the separation section, a deethanizer first separation configuration is selected as the optimal solution, and the acetylene hydrogenation is carried out after deethanization. This last issue is due to molar fractions of C_2H_2 and C_2H_4, which are major variables for the acetylene reactor. These component mole fractions increase after deethanization, and consequently, the hydrogenation process is more selective toward the acetylene hydrogenation reaction. Within the metathesis section, the reactor output stream is sent to the depropylenizer column (DC8), i.e., butenes are separated first.

On the other hand, the EU and Argentina price scenarios provide the same optimal configuration, which is different from the previously analyzed scenarios. Ethane and propane prices are the same in the EU, but ethane price is 16 % higher than propane price in Argentina. The optimal solution includes one steam cracking furnace for ethane and one for propane. A propane dehydrogenation unit based on the Cr catalyst is selected, as it is the lowest cost

Table 2
Initial process scheme.

Equipment	DC1	DC2	DC3	AR	DC7	DC8
Task	H_2C_1/C_2C_3 C_4^+	C_2/C_3 C_4^+	C_3/C_4^+	$H_2C_1C_2^x$ C_3 C_4^+	Et/Pr	Et Pr/C_4^+

Table 3
Summary of iterations with the L-bOA algorithm (USA price scenario).

Iteration/Subproblem	Objective (MM$)	Binary vars.	Continuous vars.	Constraints	Cpu time (s)
NLP 1 (CONOPT, Set Covering)	1376	-	38608	38868	479
Master MILP 1 (CPLEX)	2413	147	86375	71805	8650
NLP 2 (CONOPT)	2132	-	36880	37578	1105
Master MILP 2 (CPLEX)	1050	147	131282	115033	21458
NLP 3 (CONOPT)	1992	-	37456	37976	1169

Table 4
Optimal scheme for the different price scenarios.

	USA	EU	Russia	Argentina
Ethane furnaces	4	1	4	1
Propane furnaces	-	1	-	1
Pt-based propane dehydrogenation	-	-	-	-
Cr-based propane dehydrogenation	-	X	-	X
Ethylene dimerization	X	-	X	-
Olefin metathesis	X	-	X	-
Demethanizer	H_2C_1/C_2	H_2C_1/C_2	H_2C_1/C_2	H_2C_1/C_2
Deethanizer	$H_2C_1C_2^a/C_3C_4^+$	$H_2C_1C_2^a/C_3$	$H_2C_1C_2^a/C_3C_4^+$	$H_2C_1C_2^a/C_3$
Depropanizer	C_3/C_4	$H_2C_1C_2^aC_3/C_4^+$	C_3/C_4	$H_2C_1C_2^aC_3/C_4^+$
Acetylene reactor	$H_2C_1C_2^x$	$H_2C_1C_2^x$	$H_2C_1C_2^x$	$H_2C_1C_2^x$
Deethylenizer	Et/Pr	-	Et/Pr	-
Depropylenizer	Et Pr/C_4^+	-	Et Pr/C_4^+	-

Table 5
Economic results of the different price scenarios.

	USA	EU	Russia	Arg
Net present value (MM$)	2132	-36	1479	1414
Investment (MM$)	1089	840	1086	1001
Revenues (MM$/year)	1241	1397	1246	1255
Raw material cost (MM$/year)	275	1015	477	506
Net income (MM$/year)	570	152	457	430

propane dehydrogenation technology we have included in the superstructure. Consequently, ethylene and butenes metathesis is not selected in the optimal scheme. Regarding the separation train, a depropanizer first configuration is selected. This fact may be due to the larger content of heavier components in the reactor output stream (33.2 % of C_3^+), as compared with the case in which only ethane steam cracking is selected (1.3 % of C_3^+). Furthermore, as in the previous price scenario, the acetylene hydrogenation is located after deethanization.

5.4. Economic results

The main economic indicators are shown in Table 5 for the different price scenarios. Economic results show that the co-production plant is profitable in three of the four price scenarios for a given plant capacity of 500,000 t/y of ethylene and 500,000 t/y of propylene. In the EU scenario, a slightly negative net present value is determined, which is in agreement with information from the literature (Boulamanti and Moya, 2017), mainly due to the high price of the raw material. USA and Russia price scenarios show similar results, as the co-production plant has the same optimal design. However, the USA price scenario results in the highest NPV (2132 MM$), being the NPV for the Russia price scenario 31% lower. This difference is due to raw material cost, as ethane price is 51% lower in the USA.

In the EU case, the margins are not high enough to operate the plant under the considered global market prices for ethylene and propylene. However, it must be noted that energy integration is not performed in the current analysis. In the last part of this section, we perform energy integration for the optimal scheme and obtain more promising results for the EU case.

Price scenarios in Argentina result in a positive NPV (1414 MM$), 34% lower than in the USA, highlighting the economic potential of producing olefins in this country, with a quite different optimal flowsheet. Despite the fact that the optimal scheme is the same in both the EU and Argentina, the associated investment is higher than the corresponding one in the EU, due to the high correction factor used for Argentina (Instituto Petroquímico Argentino (IPA), 2018).

Furthermore, a comparison between producing propylene through metathesis and through PDH indicates that the former alternative requires a higher investment, for instance, in the EU capital cost is 23 % lower than in the USA. Olefin metathesis implies a higher ethylene production for the further conversion of this olefin into propylene, the USA plant produces 95 % more ethylene than the EU one. It also includes reactors for C4 hydrogenation, dimerization, isomerization and metathesis reaction, and an additional separation train to purify propylene. However, this investment increase allows taking advantage of the current low ethane price.

Finally, the potential economic improvement of simultaneous optimization and heat integration in the optimal plant configuration has been assessed for each price scenario. Multi-utilities are considered (Duran and Grossmann, 1986), and smoothing functions have been included to represent the max operators to avoid model discontinuities (Dowling and Biegler, 2015). In this particular case, one heating utility and four cooling utilities are available. In this way, we formulate the corresponding mathematical programming problem to perform the simultaneous optimization and heat integration for every price scenario. Numerical results (Table 6) show that a significant improvement of the NPV by 628 % and 21 %

Table 6
NPV in the optimal scheme with heat integration.

	USA	EU	Russia	Arg
NPV in optimal scheme with heat integration (MM$)	2199	190	1526	1715
Increase respect to base case study (%)	3.1	627.8	3.2	21.3

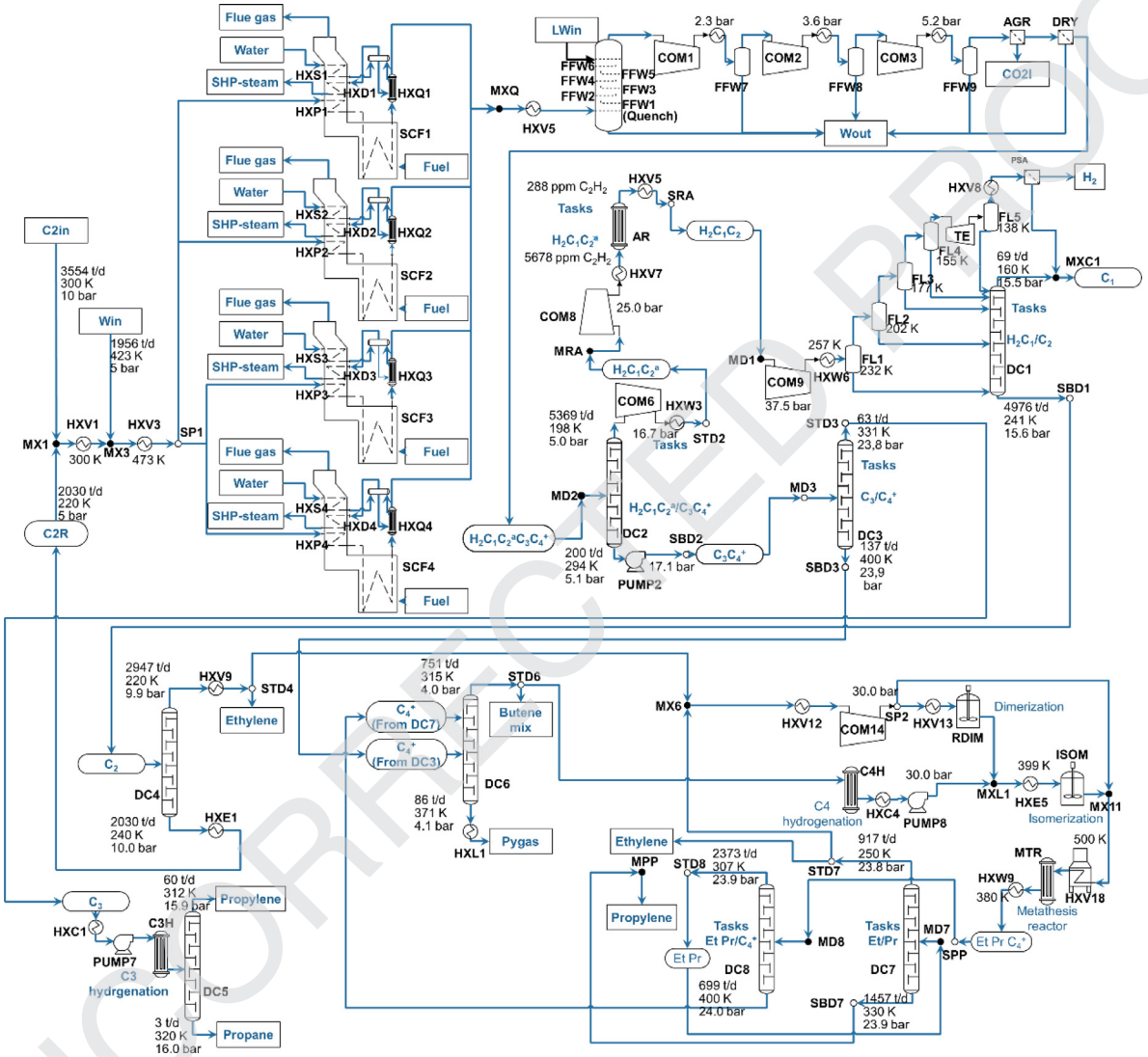

Fig. 6. Optimal plant design for the USA price scenario.

can be achieved for the European and Argentinean price scenarios, respectively. Moreover, heat integration turns the olefin plant profitable in the EU case study. On the other hand, the simultaneous optimization and heat integration for the USA and Russian price scenarios (Table 6) show potential NPV values increase of only around 3 % each. As utility prices depend on natural gas price (Ulrich and Vasudevan, 2006), this low objective value improvement can be associated to the low gas prices in these countries.

5.5. Optimal operating conditions

In this section we discuss the optimal design and operating conditions for the USA price scenario (Fig. 6). Total ethane feed to steam cracking reactors is 5632 t/d, which includes fresh ethane and ethane recycle. Four steam cracking furnaces are selected in the optimal scheme. The alkane feed is distributed equally between them since these reactors have the same size (125 MW). In each furnace, the reactive feed is preheated up to 950 K, and the cracking reaction takes place at 1100 K.

A natural gas stream of 249 t/d is used as fuel gas for each furnace, with a 10 % air excess. Also, energy integration allows recovering heat and producing 7108 t/d of high-pressure steam (110 bar), considering the contribution of all furnaces. When this steam is expanded in turbines, it is possible to produce 67 MW of electrical energy, which is mainly used as driver for the cracked gas compressor. A deethanization stage first is selected in the separation train configuration. This column has negligible propylene content (3 ppm) in the top stream, which is sent to an acetylene hydrogenation reactor, and ethane mole fraction is close to zero in the bottom stream, which is sent to a depropanizer. The acetylene hydrogenation reactor has an overall conversion of 99 % for acetylene and hydrogen consumption is 8 t/d. The outlet stream is fed to a demethanization column. Furthermore, 199 t/d of H_2 is purified in a Pressure Swing Adsorption (PSA) process, representing 86

% of its production in the crackers. In the metathesis section, 2350 t/d of ethylene is fed, from which 99 % comes from the C2-splitter top stream and the rest from a recycled stream. A significant portion of ethylene feed is converted into 1-butene via dimerization (50 %), representing 66 % of C4 olefins that are fed to the metathesis reactor (the remaining C4 olefins come from C4 hydrogenation). In the reactive mixture stream entering to the metathesis reactor, ethylene/butenes molar ratio is 2.14 and its input temperature is 500 K. This reactor operates adiabatically to produce 1457 t/d of propylene.

6. Conclusions

In this work, we have proposed a superstructure optimization approach for the optimal design of an ethylene and propylene coproduction plant. This problem is relevant due to the economic advantages of using NGLs for olefin production in the current context of shale gas revolution and the consequent reduction of naphtha cracking, which led to propylene production decrease. Rigorous models are formulated for most of the process units including distillation columns, compressors, turboexpanders, and other equipment. It is worth noting that rigorous modelling of units is not frequently encountered in the literature for large scale optimization problems, as the one analyzed in this work. We represent the superstructure with a Generalized Disjunctive Programming (GDP) model, in which the presence of process units is associated to Boolean variables. The objective function is net present value (NPV) maximization, subject to general equations, disjunctions for units, disjunctions for the state-equipment-network (SEN) representation of distillation columns and alternative acetylene reactor configurations, as well as logical equations. To solve the complex GDP model, we have carried out a custom implementation of the L-bOA algorithm in GAMS. In our case study, we consider a plant capacity of 500,000 t/y of ethylene and 500,000 t/y of propylene. We formulate a superstructure that includes ethane and propane steam cracking, propane dehydrogenation, and metathesis as potential technologies for ethylene and propylene production. We analyze different price scenarios by considering raw material and utility costs for different countries: USA, European Union, Russia and Argentina. We consider ethylene and propylene global prices.

Numerical results show that ethane and propane prices are the most important factor that impact the profitability of the process and the final process configuration scheme. The combination of ethane steam cracking, olefin metathesis and ethylene dimerization is the most profitable configuration under low ethane price scenarios (USA and Russia). In contrast, the combination of ethane and propane steam cracking together with propane dehydrogenation is the optimal solution when propane price is on the order of ethane price (EU and Argentina). It is also worth noting that numerical results show that different plant configurations can be optimal depending on the price scenario, and this was encountered through the proposed solution algorithm. Finally, we perform simultaneous optimization and heat integration for each price scenario optimal scheme. Similar results have been obtained, except for the case of the EU, whose NPV increases in 628 %, mainly associated to its high natural gas price. As part of future work, a multi-objective optimization problem will be formulated to include an environmental objective function, as well as the NPV.

Uncited references

IBM Corp., IBM 2009, Instituto Petroquímico Argentino (IPA) 2018, Maxwell and Bonnell, 1957

Declaration of Competing Interest

The authors declare that they have no known competing financial interests or personal relationships that could have appeared to influence the work reported in this paper.

CRediT authorship contribution statement

H.A. Pedrozo: Software, Investigation, Writing - original draft. **S.B. Rodriguez Reartes:** Software, Investigation, Writing - original draft. **A.R. Vecchietti:** Conceptualization, Methodology, Writing - review & editing. **M.S. Diaz:** Conceptualization, Investigation, Methodology, Supervision, Funding acquisition, Project administration, Writing - review & editing. **I.E. Grossmann:** Conceptualization, Methodology, Supervision, Funding acquisition, Writing - review & editing.

Acknowledgments

Support is acknowledged by Consejo Nacional de Investigaciones Científicas y Tecnológicas (Grant no. PIP-2015–11220150100742), Agencia Nacional de Promoción Científica y Tecnológica (Grant no. PICT-2015–3512) and Universidad Nacional del Sur (Grant no. PGI 24/M141). Support is also acknowledged by the Institute for the Design of Advanced Energy Systems (IDAES), U.S. Dept. Energy, Office of Fossil Energy.

Supplementary materials

Supplementary material associated with this article can be found, in the online version, at doi:10.1016/j.compchemeng.2021.107295.

References

Akah, A., Al-Ghrami, M., 2015. Maximizing propylene production via FCC technology. Appl. Petrochem. Res. 5, 377–392.
Ali, M.A., Ahmed, S., Al-Baghli, N., Malaibari, Z., Abutaleb, A., Yousef, A., 2019. A comprehensive review covering conventional and structured catalysis for methanol to propylene conversion. Catal. Lett. 149, 3395–3424. doi:10.1007/s10562-019-02914-4.
Andersen, F.E., Diaz, M.S., Grossmann, I.E., 2013. Multiscale strategic planning model for the design of integrated ethanol and gasoline supply chain. AIChE J. 59, 4655–4672.
Baker, I., 2018. Polypropylene, in: Fifty Materials That Make the World. Springer, pp. 169–173.
Biegler, L.T., Grossmann, I.E., Westerberg, A.W., 1997. Systematic Methods of Chemical Process Design. Prentice Hall PTR, New Jersey.
Borralho, F.J.O., 2013. Detailed Modelling and Optimisation of an Ethylene Plant. Master's thesis. Instituto Superior Técnico, Lisboa.
Boulamanti, A., Moya, J.A., 2017. Production costs of the chemical industry in the EU and other countries: ammonia, methanol and light olefins. Renew. Sustain. Energy Rev. 68, 1205–1212.
Cavani, F., Ballarini, N., Cericola, A., 2007. Oxidative dehydrogenation of ethane and propane: how far from commercial implementation? Catal. Today 127, 113–131. doi:10.1016/j.cattod.2007.05.009.
Charles, N., 2019. Total eyes shale oil for growth in Argentina on concern of low gas prices [WWW document]. URL https://www.spglobal.com/platts/en/market-insights/latest-news/oil/092719-total-eyes-shale-oil-for-growth-in-argentina-on-concern-of-low-gas-prices (accessed 2.1.20).
Chen, Q., Johnson, E.S., Siirola, J.D., Grossmann, I.E., 2018. Pyomo. gdp: disjunctive models in python. Comput. Aided Chem. Eng. 889–894.
Chin, S.Y., Radzi, S.N.R., Maharon, I.H., Shafawi, M.A., 2011. Kinetic model and simulation analysis for propane dehydrogenation in an industrial moving bed reactor. World Acad. Sci. Eng. Technol. 52, 183–189.
Cohen, 2019. Argentina – equity research [www document]. URL https://cohenmediamanager.prod.ingecloud.com/Handlers/BaseStreamer.ashx?id=i5823 (accessed 8.1.20).
Cozad, A., Sahinidis, N.V, Miller, D.C., 2014. Learning surrogate models for simulation-based optimization. AIChE J. 60, 2211–2227.
Delpino, C., Diaz, M.S., 2014. Challenges and opportunities for chemical industry in argentina. Chem. Eng. Prog. 2, 51–56.
Diaz, M.S., Bandoni, J.A., 1996. A mixed integer optimization strategy for a large scale chemical plant in operation. Comput. Chem. Eng. 20, 531–545.
Dowling, A.W., Biegler, L.T., 2015. A framework for efficient large scale equation-oriented flowsheet optimization. Comput. Chem. Eng. 72, 3–20.

Drud, A.S., 1994. CONOPT—a large-scale GRG code. ORSA J. Comput. 6, 207–216.
Duran, M.A., Grossmann, I.E., 1986. Simultaneous optimization and heat integration of chemical processes. AIChE J. doi:10.1002/aic.690320114.
Forestière, A., Olivier-Bourbigou, H., Saussine, L., 2009. Oligomerization of monoolefins by homogeneous catalysts. Oil Gas Sci. Technol. l'IFP 64, 649–667.
Gao, Y., Neal, L., Ding, D., Wu, W., Baroi, C., Gaffney, A.M., Li, F., 2019. Recent advances in intensified ethylene production - a review. ACS Catal. doi:10.1021/acscatal.9b02922.
GlobalPetrolPrices.com, 2019. Argentina electricity prices [www document]. URL https://www.globalpetrolprices.com/Argentina/electricity_prices/ (accessed 4.1.20).
Gong, J., You, F., 2018. A new superstructure optimization paradigm for process synthesis with product distribution optimization: application to an integrated shale gas processing and chemical manufacturing process. AIChE J. 64, 123–143. doi:10.1002/aic.15882.
Green, D.W., Perry, R.H., 2007. Perry's chemical, Perrys' chemical engineers' handbook. https://doi.org/10.1036/0071511245
IBM Corp., IBM, 2009. V12. 1: user's manual for CPLEX. Int. Bus. Mach. Corp., 12, p. 481.
Instituto Petroquímico Argentino (IPA), 2018. Boletín informativo IPA.
Jenkins, S., 2012. Shale gas ushers in ethylene feed shifts: growth in North American ethane cracking has wider effects for the CPI, while some companies look to harness methane for ethylene. Chem. Eng. 119, 17–20.
Jiang, W., Huang, R., Li, P., Feng, S., Zhou, G., Yu, C., Zhou, H., Xu, C., Xu, Q., 2016. Metathesis and isomerization of n-butene and ethylene over WO3/SiO2 and MgO catalysts: thermodynamic and experimental analysis. Appl. Catal. A Gen. 517, 227–235.
Kocis, G.R., Grossmann, I.E., 1989. A modelling and decomposition strategy for the minlp optimization of process flowsheets. Comput. Chem. Eng. 13, 797–819. doi:10.1016/0098-1354(89)85053-7.
Koempel, H., Liebner, W., 2007. Lurgi's methanol to propylene (MTP®) report on a successful commercialisation. Studies in Surface Science and Catalysis. Elsevier, pp. 261–267.
Koeppel, R.A., Wehrli, J.T., Wainwright, M.S., Trimma, D.L., Cant, N.W., 1994. Selective hydrogenation of C4-alkynes over a copper on silica catalyst. Appl. Catal. A Gen. 120, 163–177.
Kong, L., Maravelias, C.T., 2020a. Expanding the scope of distillation network synthesis using superstructure-based methods. Comput. Chem. Eng. 133. doi:10.1016/j.compchemeng.2019.106650.
Kong, L., Maravelias, C.T., 2020b. Generalized short-cut distillation column modeling for superstructure-based process synthesis. AIChE J. 66. doi:10.1002/aic.16809.
Lavrenov, A.V, Saifulina, L.F., Buluchevskii, E.A., Bogdanets, E.N., 2015. Propylene production technology: today and tomorrow. Catal. Ind. 7, 175–187.
Lee, S., Logsdon, J.S., Foral, M.J., Grossmann, I.E., 2003. Superstructure optimization of the olefin separation process. Computer Aided Chemical Engineering. Elsevier, pp. 191–196.
Maddah, H.A., 2018. A comparative Study between propane dehydrogenation (PDH) technologies and plants in Saudi Arabia. Am. Sci. Res. J. Eng. Technol. Sci. 45, 49–63.
Mansoornejad, B., Mostoufi, N., Jalali-Farahani, F., 2008. A hybrid GA–SQP optimization technique for determination of kinetic parameters of hydrogenation reactions. Comput. Chem. Eng. 32, 1447–1455.
Maxwell, J.B., Bonnell, L.S., 1957. Derivation and precision of a new vapor pressure correlation for petroleum hydrocarbons. Ind. Eng. Chem. 49, 1187–1196.
Mazoyer, E., Szeto, K.C., Merle, N., Norsic, S., Boyron, O., Basset, J.-M., Taoufik, M., Nicholas, C.P., 2013. Study of ethylene/2-butene cross-metathesis over WH/Al2O3 for propylene production: effect of the temperature and reactant ratios on the productivity and deactivation. J. Catal. 301, 1–7.
Mencarelli, L., Chen, Q., Pagot, A., Grossmann, I.E., 2020. A review on superstructure optimization approaches in process system engineering. Comput. Chem. Eng., 106808.
Mol, J.C., 2004. Industrial applications of olefin metathesis. J. Mol. Catal. A Chem. 213, 39–45.
Narváez-García, A., Zavala-Loría, J.C., Ruiz-Marín, A., Canedo-López, Y., 2017. Short-cut methods for multicomponent batch distillation. Distill. Innov. Appl. Model. 31.
Nawaz, Z., 2015. Light alkane dehydrogenation to light olefin technologies: a comprehensive review. Rev. Chem. Eng. 31, 413–436.
Novak, Z., Kravanja, Z., Grossmann, I.E., 1996. Simultaneous synthesis of distillation sequences in overall process schemes using an improved MINLP approach. Comput. Chem. Eng. doi:10.1016/0098-1354(95)00240-5.
Ondrey, G., 2014. Making propylene on-purpose. Chem. Eng. 121, 13.
Ondrey, G., 2004. Pushing propylene production. Chem. Eng. 111, 20–24.
Onel, O., Niziolek, A.M., Floudas, C.A., 2016. Optimal production of light olefins from natural gas via the methanol intermediate. Ind. Eng. Chem. Res. 55, 3043–3063.
Pedrozo, H.A., Rodriguez Reartes, S.B., Chen, Q., Diaz, M.S., Grossmann, I.E., 2020. Surrogate-model based MILP for the optimal design of ethylene production from shale gas. Comput. Chem. Eng. 141. doi:10.1016/j.compchemeng.2020.107015.
Qian, X., Jia, S., Luo, Y., Yuan, X., Yu, K.-T., 2015. Selective hydrogenation and separation of C3 stream by thermally coupled reactive distillation. Chem. Eng. Res. Des. 99, 176–184.
Raman, R., Grossmann, I.E., 1991. Relation between MILP modelling and logical inference for chemical process synthesis. Comput. Chem. Eng. doi:10.1016/0098-1354(91)87007-V.
Rodríguez, M., Diaz, M.S., 2007. Dynamic modelling and optimisation of cryogenic systems. Appl. Therm. Eng. doi:10.1016/j.applthermaleng.2006.02.044.
Rosenthal, R.E., 2014. GAMS—A User's Guide. GAMS Development Corporation, Washington, DC.
Ryu, J., Kong, L., Pastore de Lima, A.E., Maravelias, C.T., 2020. A generalized superstructure-based framework for process synthesis. Comput. Chem. Eng. 133. doi:10.1016/j.compchemeng.2019.106653.
Sattler, J.J.H.B., Ruiz-Martinez, J., Santillan-Jimenez, E., Weckhuysen, B.M., 2014. Catalytic dehydrogenation of light alkanes on metals and metal oxides. Chem. Rev. 114, 10613–10653.
Schulz, E., Diaz, S., Bandoni, A., 2000. Interaction between process plant operation and cracking furnaces maintenance policy in an ethylene plant. Comput. Aided Chem. Eng. doi:10.1016/S1570-7946(00)80083-8.
Schulz, E.P., Diaz, M.S., Bandoni, J.A., 2005. Supply chain optimization of large-scale continuous processes. Comput. Chem. Eng. 29, 1305–1316.
Siirola, J.J., 2014. The impact of shale gas in the chemical industry. AIChE J 60, 810–819. doi:10.1002/aic.14368.
Smith, J.M., Van Ness, H.C., 1987. Introduction to Chemical Engineering Thermodynamics, 4th ed. ed. McGraw-Hill, New York.
Stangland, E.E., 2018. Shale gas implications for C_2 -C_3 olefin production: incumbent and future technology. Annu. Rev. Chem. Biomol. Eng. doi:10.1146/annurev-chembioeng-060817-084345.
Tian, P., Wei, Y., Ye, M., Liu, Z., 2015. Methanol to olefins (MTO): from fundamentals to commercialization. Acs Catal 5, 1922–1938.
Trespalacios, F., Grossmann, I.E., 2014. Review of mixed-integer nonlinear and generalized disjunctive programming methods. Chemie Ing. Tech. 86, 991–1012.
Türkay, M., Grossmann, I.E., 1996. Logic-based MINLP algorithms for the optimal synthesis of process networks. Comput. Chem. Eng. 20, 959–978.
U.S. Energy Information Administration, 2019. The United States expands its role as world's leading ethane exporter [www document]. URL https://www.eia.gov/todayinenergy/detail.php?id=38232 (accessed 11.1.19).
U.S. Energy Information Administration, 2013. Technically recoverable shale oil and shale gas resources: an assessment of 137 shale formations in 41 countries outside the United States [www document]. URL www.eia.gov/analysis/studies/worldshalegas/ (accessed 6.1.13).
Ulrich, G.D., Vasudevan, P.T., 2006. How to estimate utility costs. Chem. Eng 113, 66–69.
Vecchietti, A., Grossmann, I.E., 2000. Modeling issues and implementation of language for disjunctive programming. Comput. Chem. Eng. 24, 2143–2155. doi:10.1016/S0098-1354(00)00582-2.
Verma, V.K., Hu, J., 2008. Low pressure olefin recovery process.
Viswanathan, J., Grossmann, I.E., 1993. Optimal feed locations and number of trays for distillation columns with multiple feeds. Ind. Eng. Chem. Res. 32, 2942–2949.
Węgrzyniak, A., Jarczewski, S., Węgrzynowicz, A., Michorczyk, B., Kuśtrowski, P., Michorczyk, P., 2017. Catalytic behavior of chromium oxide supported on nanocasting-prepared mesoporous alumina in dehydrogenation of propane. Nanomaterials 7, 249.
Wilding, W.V., Rowley, R.L., Oscarson, J.L., 1998. DIPPR® project 801 evaluated process design data. Fluid Phase Equilib 150, 413–420.
Yeomans, H., Grossmann, I.E., 2000. Disjunctive programming models for the optimal design of distillation columns and separation sequences. Ind. Eng. Chem. Res. 39, 1637–1648.
Yeomans, H., Grossmann, I.E., 1999a. A systematic modeling framework of superstructure optimization in process synthesis. Comput. Chem. Eng. 23, 709–731. doi:10.1016/S0098-1354(99)00003-4.
Yeomans, H., Grossmann, I.E., 1999b. Nonlinear disjunctive programming models for the synthesis of heat integrated distillation sequences. Comput. Chem. Eng. 23, 1135–1151. doi:10.1016/S0098-1354(99)00279-3.
Zimmermann, H., Walzl, R., 2009. Ullmann's Encyclopedia of Industrial Chemistry. Ethylene. John Wiley & Sons, Inc., New York.